THE ANALYSIS OF ALUMINUM AND SODIUM IN IGNEOUS ROCKS BY INDUCED RADIOACTIVITY

A Thesis

Presented to the

Faculty of Graduate Studies and Research

University of Manitoba

In Partial Fulfillment

of the Requirements for the Degree

Master of Science

Allan Charles Turnock

May, 1956.

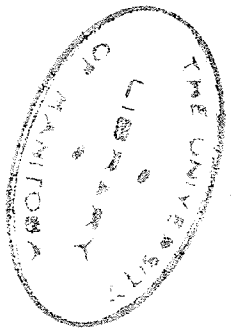

THE ANALYSIS OF ALUMINUM AND SODIUM IN IGNEOUS ROCKS BY INDUCED RADIOACTIVITY

by

Allan Charles Turnock

ABSTRACT

The operation and calibration of a scintillation counter is described; and the theory and method of activation analysis is discussed.

The analysis for the Al content of a series of chemically analysed igneous rocks and bauxites is found to be within

(a) for igneous rocks $15 \pm 0.9\%$ Al_2O_3

The analysis for the Na content of a series of chemically analysed rocks is found to be within $2 \pm 0.3\%$ Na_2O.

The equipment is easily converted into an alpha counter by changing the scintillator. It is shown that the alpha activity of less than 1 gram of zircons can be detected.

TABLE OF CONTENTS

PART I

OPERATION OF SCINTILLATION COUNTER

PART II

METHOD

Page

PART V

LIST OF TABLES

Page

PART II

PART III

PART IV

LIST OF ILLUSTRATIONS

Page

INTRODUCTION AND ACKNOWLEDGEMENTS

Induced radioactivity analysis has been gaining favor because of its ease and rapidity, and also because the counting equipment is more commonly available. If a monoenergenic source were available, even more work would be done. Recently several authors (Meinke (1955) and Muehlahuse and Thomas (1950)) have applied the method, in combination with chemical separation, to trace elements, with encouraging results.

The object of this research program has been to find a fast, dry, method for Si, Al and Na in rocks, that could speed research on fundamental geological problems.

The assistance of Dr. K.I. Roulston, Dr. W.E. Turchinetz, R.B. Moore, and A. Petkau with electronic troubles and for helpful discussions is gratefully acknowledged.

PREVIOUS WORK

The program has been conducted by Dr. G.M. Brownell, with the aid of grants from the Geological Survey of Canada, and the advice of Dr. R.W. Pringle and Dr. K.I. Roulston of the Department of Physics. K. Bramadat set up the apparatus and did the preliminary experiments during 1952-54. R.A. Knutson worked out the method for Si, and suggested the method for Al in 1953-54. H. Cohen started the experiments on Na. H. Kowalik improved the arrangement of the apparatus.

PART I

OPERATION OF A SCINTILLATION COUNTER

APPARATUS

The scintillation counter may be conveniently divided into its component parts, each one performing its operation and passing the results on to the next:-

1. Voltage regulator
2. Power supply
3. Scintillator (or phosphor)
4. Photomultiplier tube
5. Cathode follower
6. Amplifier
7. Discriminator
8. Counter
9. Oscilloscope

The apparatus is shown in fig. 1 and fig. 2.

The equipment operates as follows: a particle or quantum with sufficient energy impinging on the scintillator

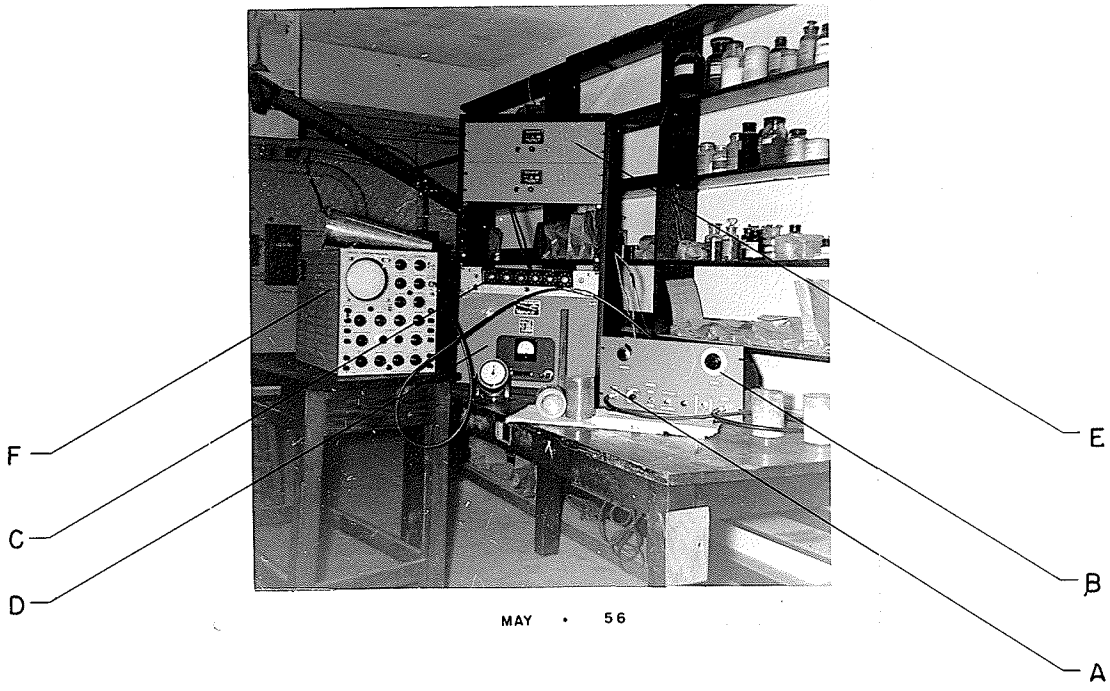

Fig. 1. Scintillation counter

A. Amplifier
B. Discriminator
C. Counter
D. Power regulator
E. Power supply
F. Oscilloscope

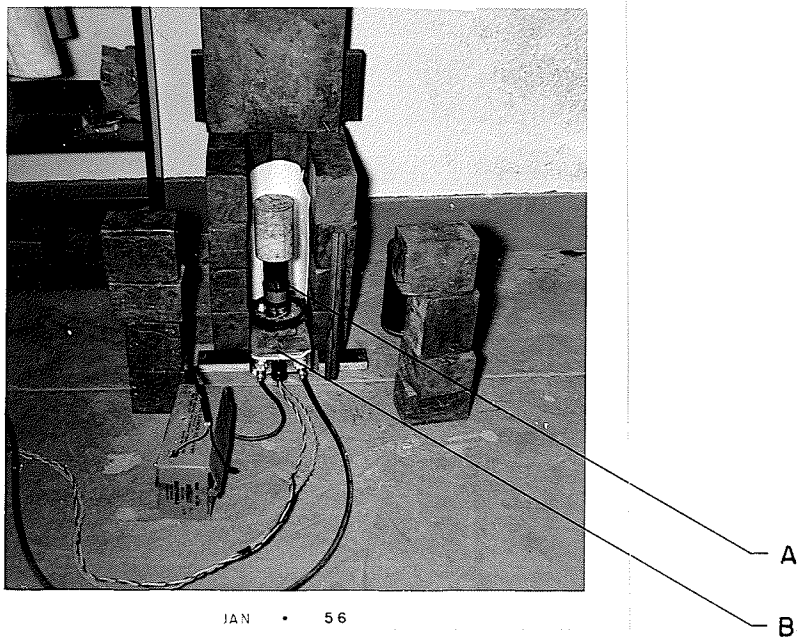

Fig. 2. Castle and detection unit

A. Photomultiplier tube

B. Base containing the cathode follower

produces a flash of light; the magnitude of this flash of light is proportional to the energy of the incident radiation, and this relationship is carried through into the discriminator. The flash of light is directed into the photomultiplier tube, where it is changed into an electronic pulse. The cathode follower records this pulse and sends it into the amplifier, which amplifies it and sends it to the discriminator. The discriminator will accept only those pulses within a desired range of amplitude. The gates are variable so that any range may be selected. The accepted pulses trigger the circuit that sends a pulse into the counter, which registers as one count. These steps will be followed in more detail.

1. Voltage regulator. A Sorenson Model 2000 S.A.C. voltage regulator takes the 110 v. A.C., 60 cycle, from the wall plug and feeds 115 v. A.C. into the power supply. This valuable piece of equipment provides a supply of current with less than 1% voltage variation.

2. Power supply. A Lambda Model 28 power regulator takes the output of the power supply and provides regulated voltages in D.C. for the circuits, and A.C. for the heater filaments in some tubes.

3. Scintillator. Radiation produces flashes of light, or scintillations, in certain substances. For gamma rays, NaI(Tl) is commonly used; but for alpha particles, ZnS(Ag) is best. The NaI(Tl) crystal used was 2'' in diameter by 2'' thick,

Harshaw mounted. The NaI(Tl) crystals are coated with a reflecting MgO layer, and mounted in an aluminum case. Bramadat (1954) describes the physical processes. The energy of the flash produced is proportional to the energy of the incident ray. However, if the type of scintillator is changed, the calibration of the instrument will be changed. The larger the crystal, the more rays will be counted, because of increased volume receiving radiation.

4. Photomultiplier tube. The face of the scintillator is placed against the face of the photomultiplier tube with a light transmitting silicone fluid contact. This contact is taped light-tight. The MgO coated sides of the scintillator are reflecting, so a scintillation must pass into the photo-multiplier tube. The scintillation produces the photoelectric effect on the cathode, yielding electrons which are focused onto a series of dynodes that multiply the number of electrons, so that an enlarged pulse emerges from the tube. This tube takes about 1000 v as there is about 100 v in each dynode step. The tube will operate between about 800 and 1300 v. An increase in voltage raises the amplitude of a pulse, but does not increase the counting rate.

5. Cathode follower. This tube picks up the pulses from the photomultiplier tube and sends them to the amplifier. It operates on voltage from the power regulator.

6. Amplifier. The pulses are amplified linearly up to a maximum output of about 80 volts.

7. Discriminator. This instrument enables the operator to count only those pulses of desired amplitude. The main adjustment is the ''bias voltage'', also called the ''trigger level'' and referred to as a bias set. Only pulses with height greater than the setting of this ''trigger level'' will pass and be counted. See fig. 3. The calibration of the discriminator is the determination of the relationship between the numbers on the dial of the bias setting and the corresponding pulse height. All pulses higher than the setting of the trigger level are counted when the discriminator works as an integral discriminator.

Switching the toggle switch on the discriminator panel changes the integral discriminator into a differential discriminator, by adding one more discriminatory operation. This is an upper limit to the trigger level. Pulse heights greater than this upper limit do not count. The distance, or energy range, between this upper limit and the lower limit, which is the trigger level of integral discriminator, is called the gate width. As shown in fig. 4, the only pulses counted are those having a pulse height that falls within the gate. Because this gate analyses the energy of the pulse, it may be called an analyser as well as a differential discriminator.

The width of the gate is variable. Turning the gate dial raises or lowers the upper limit in respect of the bias

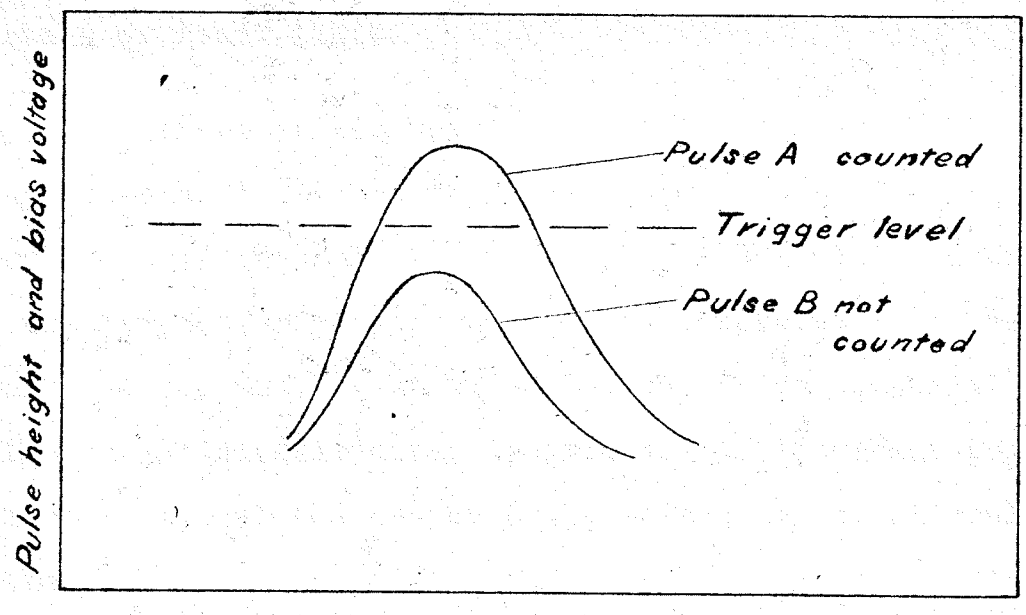

Fig.3 Integral pulse height discrimination diagram

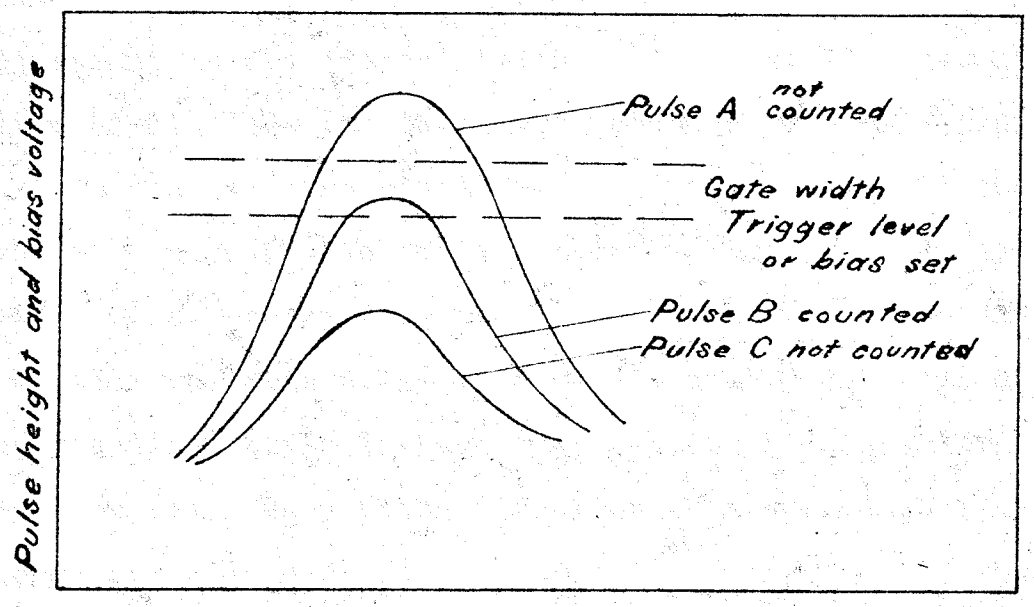

Fig.4 Differential pulse height discrimination diagram

voltage or lower limit.

Those pulses which are within the acceptable energy range of the discriminator trigger the output circuit, and come out as pulses of equal height. On the oscilloscope, this is the largest, strongest pulse; also there will be some low energy noise, and stray low energy cancelled pulses if the differential discriminator is in use. An important point to remember is that the output pulse energy may be slightly different between integral and differential discriminators. This may affect the counting rate in the counter, which has a ''sensitivity set'' adjustable to the input pulse amplitude.

8. Counter. The counter is a glow transfer counter, Atomic Instrument Co., Model 162. It records the counts on glow tubes. The set-up is like a house meter. The important adjustment is the ''sensitivity set'', a small screw at the right back. This is, in effect, another integral discriminator. This setting is very sensitive, a quarter turn will change it from zero through the maximum counting rate. If it is set too low, the low energy noise will count. It should be set about 1 v below the main pulse voltage, so that drift will not affect the counting rate. To test this setting find the maximum counting rate, then using differential discriminator, close the gate. The counting rate should decrease until, when the gate is at zero, the counting rate approaches zero. Make slight adjustments to the sensitivity set until this takes place.

9. Oscilloscope. This is an auxiliary piece of equipment that has two uses, namely ''pulse analysis'' and ''trouble shooting''.

Pulse analysis. The pulse is put on the screen of the oscilloscope by adjusting the various knobs. The beginner will require a demonstration of these adjustments. The height of the pulse will be proportional to the energy or voltage, and the length of the pulse is proportional to its time of duration. The energy of a pulse may be found in two ways. A pulse of known energy may be run into the oscilloscope, either at the same time or separately, and the heights compared; or the pulse may be calibrated into voltage by changing the appropriate knob from ''signal'' to ''calibrate voltage''. First mark the pulse height directly on the screen with ink. Then change to ''calibrate voltage'', and adjust it until there is a vertical line the same height as the pulse mark. Then the dial gives the voltage of the pulse.

To find the energy of the gamma rays, plug the oscilloscope into the amplifier output, and compare the pulse height to one of known energy; e.g. Cs with a strong line at the top of its spectrum with an energy of 0.662 Mev. To find the voltage of the output pulse of the discriminator, plug the oscilloscope into the discriminator output; and calibrate as to voltage.

Trouble shooting. To find a breakdown, the oscilloscope

will show the output of each unit, and thereby locate the trouble.

STANDARD PROCEDURE WITH APPARATUS

1. Plugging in. The wall plug should be left in, and all the units turned off individually. Turn them on in order. First switch on the Sorenson voltage regulator. The needle will show about half voltage until it warms up. In a minute the needle will jump to 115, the output voltage; then the power supply may be turned on. Give it a couple of minutes, or until all the tubes have a steady glow. Now switch on the discriminator. It may take an hour or more until it is steady because all electronic equipment drifts during warm-up. Do not turn them all on at once, because it is harmful to switch cold equipment onto maximum load. Turn off in reverse order.

2. Cooling. The transformers and tubes give off considerable heat, of which an excess may harm the tubes or impair their operation. The units are spread out so that air can circulate among them. If too much heat collects, a fan is required. When the equipment is not to be used for several days, turn it off.

3. High voltage to photomultiplier tube. This is supplied by 3 or 4 dry batteries. Very little current is drawn. If light is allowed to enter the photomultiplier tube when the high voltage is on, it will be ruined. The contact with the scintillator is usually well taped, and should be light tight;

however, as a precaution, turn off the high voltage before opening the can which houses the photomultiplier and scintillator.

CALIBRATION

1. Check ''sensitivity set'' on the counter. This is a very sensitive adjustment, which may drift off its setting; but it can be checked in a few minutes and this should be done every day. Place a source, e.g. the Cs 137, over the scintillator. Turn on the differential discriminator, and adjust the bias until a fast counting rate is found. Adjust the sensitivity set until the maximum counting rate is obtained. Now close the gate. The counting rate will decrease. When the gate is at zero, the counting rate should be zero, or very slow; adjust the sensitivity set until it is. Now open the gate, the counting rate should increase again. The following explains what happens. Besides the main pulse coming out of the discriminator, there are some low energy noise pulses too, which are tube noise and cancelled pulses. The ''sensitivity set'' acts as another integral discriminator, and its job is to discriminate out these low energy noises. If it is set too low, it will allow these noises to count; then the gate will not zero. If it is set too high, there will be no counting. The setting is very touchy, a fraction of a turn sets it off or on. See Fig. 5.

2. Calibration of discriminator. This is the most important adjustment of the instrument, relating the setting

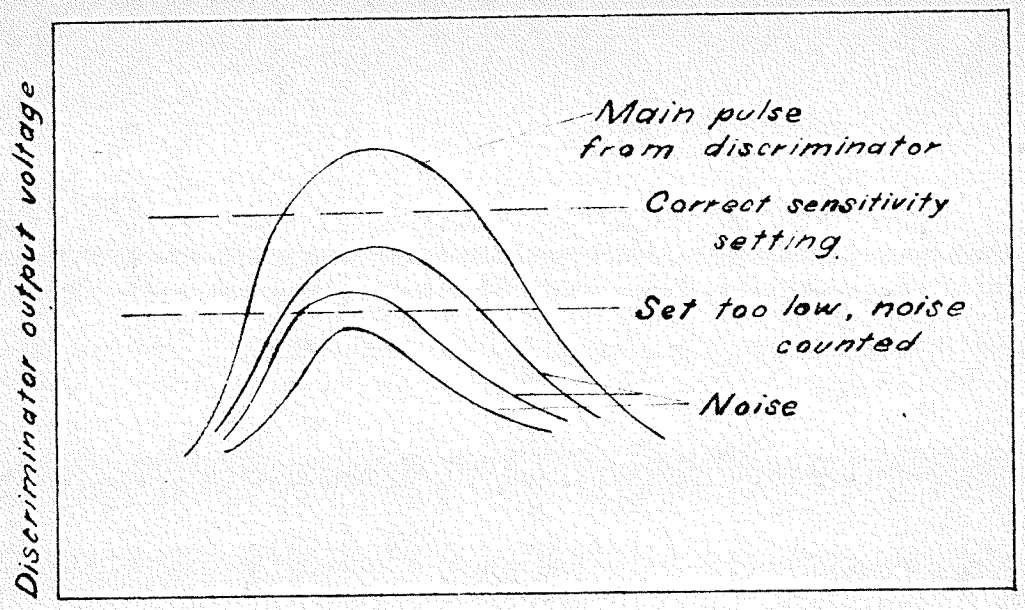

Fig.5 Counter sensitivity set pulse discrimination diagram

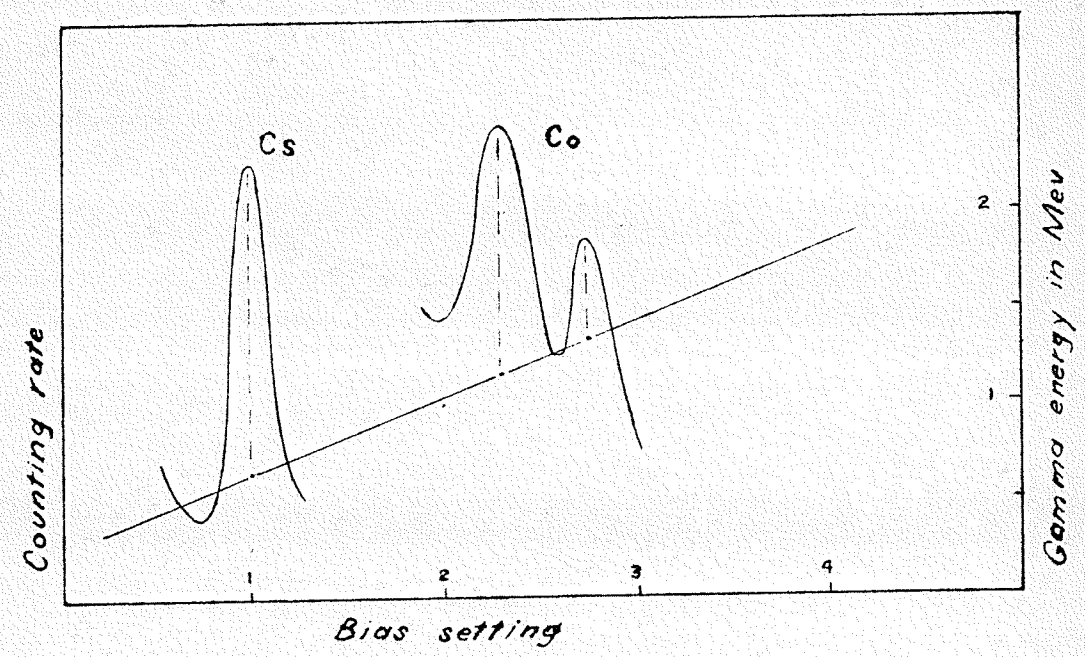

Fig.6 Calibration of discriminator

of the bias to the energy of the incident radiation. Place the Cs source over the scintillator. Cs has only one gamma ray, at an energy of 0.662 Mev. and at this energy level we will find a distinct photoelectric peak. First the location of the peak may be found roughly by using the integral discriminator. Find at low bias setting a fast counting rate. Now increase the bias. The counting rate will decrease slowly until the peak is passed, suddenly it will decrease noticeably, and fall off to a very slow rate. The fall off is the high side of the peak. Change to differential discriminator, and close the gate to its narrowest practical width; that will be one-half or 1 volt, increasing with increased amplification. Now take readings at regular bias settings across the peak. For the Cs source a 30 sec. count is satisfactory. Take a piece of squared graph paper, mark the bias settings as abcissae and the counting rate as ordinate. The resulting graph should show a sharp peak, as in Fig. 6. The position of this peak on the bias corresponds to an energy of 0.662 Mev. in this figure it is at 1.0. The next step is to locate the peaks of other sources, which may be obtained from the Physics Department. The Zn 65 has a small peak at 1.10 Mev. Co 60 has two peaks at the end of its spectrum, at 1.17 and 1.33 Mev, as shown in Fig. 6. Now the calibration line may be drawn. Plot the energies of the peaks against the bias settings. The line should be nearly straight. This calibration can be applied to both integral and differential discriminators. However, it is changed by alteration of the high voltage on the photo-

multiplier or change of amplification or change of phosphor.

3. Calibration of Gate. The gate is easily calibrated with a pulse generator. A pulse is moved across the gate width; when the upper limit is reached the counting stops, and the pulse is left sitting just above the gate. Then the bias is turned up so that the gate width moves across the pulse. The change in the bias setting is the gate width. If desired, the gate width can be related to pulse energy through the bias calibration.

4. Linearity of Amplifier. The amplifier should be close to linear. Locate the peak of Cs at each amplifier setting, plot the bias setting against amplifier setting. Note that the gate width must be doubled with each increase in amplification.

5. Resolution power of photomultiplier tube. The efficiency of the photomultiplier tube in producing a pulse exactly proportional to the energy of the scintillation is called the resolution. Take the Cs peak and measure the width half way up. Divide this width by the bias voltage at the centre of the peak. This ratio is the resolution. With it record the high voltage on the photomultiplier.

PART II

METHOD

OUTLINE OF METHOD

1. Preparation of sample.
   (a) Crush to 1/4 inch size.
   (b) Weigh 300 g. sample into container.
2. Irradiate with slow neutrons.
   (a) For Al, 8 minutes.
   (b) For Na, 16 hours.
3. Measure resultant gamma activity, using scintillation counter.
4. Graphically analyse the radioactive decay, and compare the initial activity of the Al component with that of a standard.

DETAILED PROCEDURE

1. Choose as a standard a chemically analysed rock of the same type as the sample. Run it alongside of the unknown, or 2 or 3 times during the day.

2. Sample preparation. Crush to approximately 1/4 inch size. Fragments must be less than 3/8 '' largest diameter to fit the thin part of the containers. Grinding is undesirable, because powders do not give as good results as crushed samples. 300 g. samples were weighed on a table balance.

3. Neutron irradiation. Po-Be sources were used.

They were kept in the plastic well in the tank of oil and water, as shown in Fig. 7, and covered with a block of paraffin. Neutrons of all energies up to 11 Mev. are emitted. Most of these are thermalized (slowed to energies of the thermal range, less than 1 ev.) by the surrounding oil and water, and the layer of paraffin. The sample is lowered on top of this. For an 11 curie source, 9.3 cm. of paraffin was used, giving a slow neutron flux on the sample of about 5×10^4 n/s/cm.^{2}, (measured by W.E. Turchinetz). For a 5 curie source, 6.0 cm. of paraffin was used, giving a flux about 4×10^4 n/s/cm.^{2}.

For Al analysis, irradiation time was 8 minutes.
For Na analysis, irradiation time was 16 hours.

4. Counting gamma activity. The sample is lifted out of the tank at the end of the irradiation period; this is also time zero on the decay graph and the point of initial activity. Stop-watch control is required. As quickly as possible, the sample is placed over the scintillator crystal, the castle lid is closed, and the high voltage to the photo-multiplier is switched on. These operations can be performed in 12 seconds. The operator then moves to the counter switch, to start the counting at t = 15 s.. The detection unit, shown in Fig. 2, is kept in a lead castle to reduce the background.

The cumulative count was read without stopping the count at 30 s., 1.0 m., and every 30 s. for the first 5 m., then every 1 m. for the next 10 m., then every 2 m. up to 35m.,

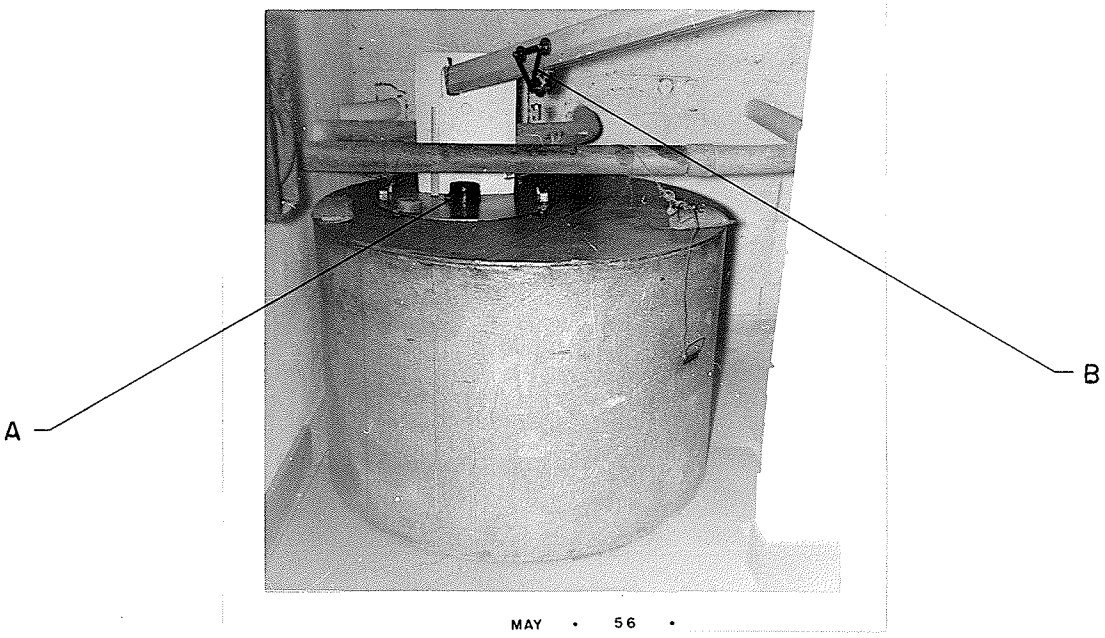

Fig. 7. Tank for holding neutron source

A. Well one foot deep.

B. Trolley for moving source out of the tank for fast neutron bombardment.

for the Al analysis. The counting for Na is described in Part IV.

5. For Al, the activity in counts per 30 seconds is plotted on semi-log paper, and the background and other interferring induced activities are subtracted as in Fig. 13. This leaves the straight line component (a) of the Al^{28} isotope having a half life of 2.3 minutes. From its initial activity the correction for Si is made, and the remaining activity is proportional to the content of Al. The Si correction is the product of the Si content and the Si activation factor. This constant is found by running a standard of Si sand, as shown in Fig. 22.

THEORETICAL CONSIDERATIONS OF METHOD

1. Comparison of initial activities. This method is not independent. It is made quantitative by comparing the induced activity of a known isotope in the sample with the same induced activity of an analysed standard. As shown in Fig. 13, the decay graph can be confidently extrapolated to zero, and for Al, the initial activities are compared.

Comparison is by far a better method than an attempt to evaluate the relationship:

$$A = \frac{w\ Av.\ f\ \sigma\ d}{M}\left(1-e^{\frac{-0.7T}{\tau}}\right)\ e^{\frac{-0.7t}{\tau}}$$

A = Activity

w = weight of element

Av. = Avogadro's no.

f = neutron flux

σ = reaction cross section

d = isotope abundance

M = atomic weight

T = Time of irradiation

t = time of decay

τ = half-life of induced activity

2. The samples must have the same geometric shape. This is necessary because in order to fulfill the conditions of comparison the same shape must be offered to the neutron irradiation and the gamma-detecting scintillator crystal. The cylindrical sample containers were made of clear plastic, with a central cavity to enable it to fit around the crystal for most efficient counting (see Fig. 8). The outside diameter is 3 1/2'', and 4 1/2'' high. The central cavity is 2 1/8'' in diameter and 2 3/8'' high. These containers, as in Fig. 8, hold 300 grams of a crushed igneous rock.

3. Sample size. To fit into the container, fragments of 1/4'' size are satisfactory. Fine crushing is not necessary; in fact, poor results were obtained from the powdered bauxite samples.

4. Sample weight. The larger the better, because the amount of induced activity is proportional to the amount of the element present, and increasing the counting rate decreases the statistical error. The amount of sample used is limited by:

Fig. 8. Sample containers

A. Central cavity

(a) the size of container that will fit in the neutron tank and over the crystal in the counting position, with easy handling, and

(b) the self absorption of gamma rays. As the sample gets thicker, absorption increases exponentially.

5. Time of irradiation. The formula for induced activity is given on page 19. The factor for radioactive build-up is $(1-e^{\frac{-0.7T}{\tau}})$. This factor is graphed in fig. 9, against T, the time of irradiation in number of half-lives. It is seen that it is the mirror image of radioactive decay. After 3 or 4 half-lives the curve is beginning to flatten out, and maximum induced activity, or saturation, is being approached.

6. Method of Irradiation. The use of Po-Be sources involves the problem of trying to thermalize efficiently the polyenergetic neutrons. When the paraffin is thick enough to thermalize the fastest neutrons, the slower ones are absorbed, leaving only a weak flux. It is difficult to avoid the fast neutron reactions taking place to some extent. They are not critical to Al analysis except for the Si, which must be corrected for. The fast neutron effect with Al, giving 9.5 min. Mg, as shown in table 1, was not evident in the decay curves of Al_2O_3, igneous rocks or bauxites (see figs. 10-21 and 26-31). These samples were irradiated through 9.3 cm of paraffin for the 10.95 curie source, and 6.0 cm paraffin for the 5 curie source. When the source was about 1/3 curie,

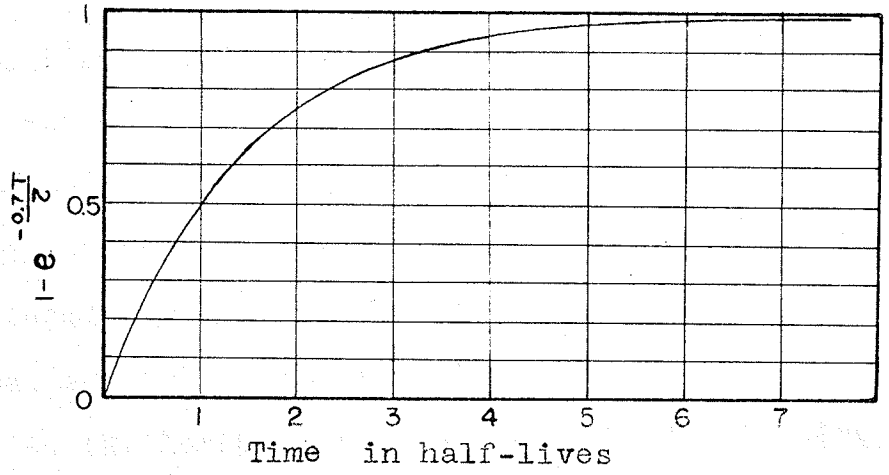

Fig.9 Radioactive build-up

3.3 cm of paraffin was used; however, the curves were poor and no conclusions could be drawn on the effect of fast neutrons.

Some information on flux density is available.

Source 10.95 curie on January 13, 1956

Alpha activity of Po	$10.95 \times 3.7 \times 10^{10}$	$= 40.5 \times 10^{10}$ a/s
Neutron emission		2.63×10^{7} n/s
Be activation efficiency		6.49×10^{-5} n/a
Calculated flux at 9.3 cm		2.4×10^{4} n/s/cm^2
Thermal neutron flux measured with		
Au (W. Turchinetz) 9.3 cm. paraffin		5×10^{4} n/s/cm^2

The thermal neutron flux is higher at about 10 cm from the source because of the effect of maximum reflection and gaseous behaviour at this distance.

The 10.95 curie source was too strong to use the related Si analysis with a 300 g sample, because the induced activity approached the maximum load of the counter.

The Po-Be type of neutron source has the following advantages over a reactor type (e.g. N.R.X. Chalk River, flux greater than 10^{11} n/s/cm^2):

(a) Low temperature. (it is 150° in N.R.X.)

(b) A large sample can be used. (the maximum size that can be placed in N.R.X. is 1 3/4'' x 3/4'')

7. Neutron capture reactions producing gamma activity. Table 1 shows the reactions that may be expected when

an igneous rock is bombarded by neutrons. It is divided into two sections to distinguish the results of fast and slow neutrons. This data was obtained from Nuclear Data, Circular of the N.B.S., and Nuclear Science Abstracts.

To a small extent, the fast neutron reactions will take place during slow neutron irradiation, because of the imperfection of the thermalization.

8. Sources of error. Most of these are too small to be calculated, most of them are compensating, and most of them are reduced in the use of a comparison method.

(a) Packing the sample in the container. Samples should be identical in volume and shape. Igneous rocks, when crushed in the same way, approach this condition for 300 g samples; however, there was small variations in fineness of crushing and density. The powdered bauxites had large differences in density, and the weight of the samples varied from 200 to 280 g. Numbers 4 and 5 were particularly fluffy, and gave lower results. The experiments on bauxites indicate that an increase of sample size of 20 g. causesan error of 8%.

(b) Weighing errors. The table balance is accurate to within 0.1 g. On a 300 g. sample, this is 0.03%.

(c) Time of neutron irradiation. The 8 m. exposure for Al approaches saturation; the activity build-up curve has flattened off (fig. 9). Therefore, errors of a few seconds are negligible. In the case of Na^{24}, with a half-life of 15 hours, the irradiation time was 16 hours. The build-up curve

TABLE I

NEUTRON CAPTURE REACTIONS PRODUCING GAMMA ACTIVITY

Isotope and abundance	Reaction	Product	Cross sect. in barns	Gamma decay
	Fast neutrons			
Si^{28} 92%	(~1Mev.n,p)	2.3m Al	0.003	1.8 Mev.
Si^{29} 5%	(~1Mev.n,p)	6.7m Al	0.0027	1.2,2.3
O^{16} 99.7%	(~1Mev.n,p)	7.3s N	0.014	6.2
Al^{27} 100%	(~1Mev.n,γ)	2.3m Al	0.0004	1.8
Al^{27} 100%	(~1Mev.n,p)	9.5m Mg	0.003	0.84,1.01
Al^{27} 100%	(~1Mev.n,a)	15 h Na	0.0006	1.38,2.76
Fe^{56} 92%	(fast n,p)	2.6h Mn	0.09	0.8,1.8,2.1
Mg^{26} 11%	(~1Mev.n,γ)	9.5m Mg	0.0006	0.84,1.01
Na^{23} 100%	(~1Mev.n,a)	12 s F	0.01	2.2
Na^{23} 100%	(~1Mev.n,γ)	15 h Na	0.0003	1.38,2.76
Na^{23} 100%	(fast n,p)	41 s Ne	0.0011	2.8
K^{41} 100%	(~1Mev.n,γ)	12.4h K	0.003	1.5
Ti^{48} 74%	(fast n,p)	1.8d Sc	0.023	0.98,1.33
Ti^{46} 8%	(fast,n,2n)	3.1h Ti	0.053	0.48,0.8
	Thermal neutrons			
Al^{27} 100%	(th n,γ)	2.3m Al	0.21	1.8
Mg^{26} 11%	(th n,γ)	9.5m Mg	0.05	0.84,1.01
Na^{23} 100%	(th n,γ)	15 h Na	0.6	1.38,2.76
K^{41} 7%	(th n,γ)	12.4h K	1.0	1.46
Ti^{50} 5.4%	(th n,γ)	6 m Ti	0.14	0.32

is steep at this time, but an error of 4 seconds would be only 0.5%.

(d) There may be a slight error, less than 1 second, in timing the removal of the sample from irradiation. This is time zero on the decay graph. Consideration of fig. 12 indicates that a timing error of 1 second would shift the curve laterally a distance less than the width of a pencil line. This is much less than the error in drawing the line, and because the timing control is better than $\pm$ 1/2 s., this error is insignificant and was not included by Knutson in his summation of error.

(e) Counting errors.

(e) 1. The statistical counting error of the photomultiplier tube is $\pm$ the square root of the number of counts.

(e) 2. There is some error in reading the moving dial which is estimated at about 0.1%

However, both these errors are directly compensated by drawing the best line between points. Knutson evaluated these errors at $\pm$ 2.1%. They are the major factors in the error of the method.

(e) 3. Electronic components, especially in the discriminator and the counter, may drift and vary the discriminator levels. This caused quite a bit of trouble during the year, and is the cause of some anomalous results. It can be the cause of systematic errors during the day.

(f) The other elements present may interfere by their induced activity, or by absorption of gamma rays, and may cause systematic errors. The results of these experiments (table 3) showed that such systematic errors did occur, because the activation constants for the basic rocks are higher than those of the acid rocks. This effect may be due to the interference of the basic elements, especially Fe and Mg. The success of this method must depend on the comparison of the sample with a similar rock type.

PART III

ALUMINUM ANALYSIS

Al ANALYSIS IN IGNEOUS ROCKS

1. The standard samples used were a suite of acid to basic igneous rocks, chemically analysed by the Minnesota Rock Analysis Laboratory. These are shown in table 2.

2. Experimental data. The decay curves of the induced activity of the igneous rocks are shown in figures 10 - 20. The curve for an Al casting and Al_2O_3 powder used by Bramadat is shown in fig. 21. The initial activity of the 2.3 m Al^{28} component is taken from the graph. However, this activity is due to more than one nuclear reaction, as considered on page 26.

The contribution of Si was determined experimentally by running a 300 g sample of Black Island silica sand, 99.33% SiO_2. The decay curve is shown in fig. 22. The initial activity was 2.8 counts/30s/g SiO_2.

The contribution of silica to the 2.3 m component is found by multiplying this activation constant by the silica content. After subtracting the silica correction, the initial activity remaining is due to the Al content, and is proportional to the amount. The activation constant, in counts/30s/g Al_2O_3, should be the same for all samples, and these are compared in table 3.

TABLE 2

UNIVERSITY OF MINNESOTA

ROCK ANALYSIS FOR INDUCED RADIATION RESEARCH

	R - 1883	R - 1791	R - 1737	R - 1738
SiO_2	77.75	67.30	65.49	64.13
Al_2O_3	12.71	15.44	14.49	16.77
Fe_2O_3	0.39	1.77	2.11	1.96
FeO	0.47	1.83	2.90	1.69
MgO	0.34	1.52	2.45	1.29
CaO	0.68	4.19	4.29	2.72
Na_2O	6.24	3.10	2.80	3.92
K_2O	0.40	3.68	3.66	5.77
H_2O^+	0.38	0.35	0.56	0.39
H_2O^-	0.13	0.07	0.05	0.19
CO_2	0.40		0.05	0.02
TiO_2	0.21	0.32	0.65	0.52
P_2O_5	0.01	0.15	0.21	0.23
MnO	0.01	0.10	0.10	0.05
SrO			0.04	0.02
BaO			0.05	0.10
S			0.01	0.01
	Sodaclase Microgranite	Granodiorite	Grandiorite	Monzonite

TABLE 2 (continued)

	R - 1751	R - 1730	R - 1803	R - 1982	R - 1989
SiO_2	58.45	56.13	54.75	49.65	49.21
Al_2O_3	15.71	17.39	12.20	13.22	14.24
Fe_2O_3	1.61	4.32	6.48	1.58	2.36
FeO	6.76	2.44	8.78	11.76	10.59
MgO	1.34	4.02	2.97	5.44	5.73
CaO	4.97	7.69	4.08	8.98	9.14
Na_2O	4.08	2.63	4.18	2.71	2.72
K_2O	3.98	0.64	1.17	0.97	0.97
H_2O^+	0.31	2.55	1.61	0.59	1.00
H_2O^-	0.08	1.64	0.15	0.18	0.19
CO_2	0.23	0.01	1.52	0.04	0.02
TiO_2	1.46	0.47	1.50	3.93	2.83
P_2O_5	0.61	0.06	0.15	0.53	0.50
MnO	0.14	0.17	0.16	0.21	0.19
SrO	--	--	--	--	--
BaO	0.14	--	0.05	--	--
S	0.07	--	0.34	0.08	0.07
	Syenite Gneiss	Dacite	Granophyric Diabase	Basalt Dike	Coarse Diabase

TABLE 2 (continued)

	R - 1988	R - 1987	R - 1767
SiO_2	49.18	41.31	38.91
Al_2O_3	13.82	12.12	6.98
Fe_2O_3	2.46	3.52	4.93
FeO	10.99	14.57	29.07
MgO	5.44	6.58	3.85
CaO	9.16	11.07	6.55
Na_2O	2.72	2.06	1.00
K_2O	0.98	0.16	0.42
H_2O^+	1.04	0.44	0.34
H_2O^-	0.20	0.06	0.07
CO_2	0.04	0.05	
TiO_2	2.99	7.04	4.70
P_2O_5	0.56	0.63	1.61
MnO	0.20	0.21	0.52
SrO			
BaO			
S	0.09	0.10	FeS_2- 0.98
	Diabase Dyke (Chill Zone)	Basalt Hornfels	Garnetiferous Ultramafic Gabbro

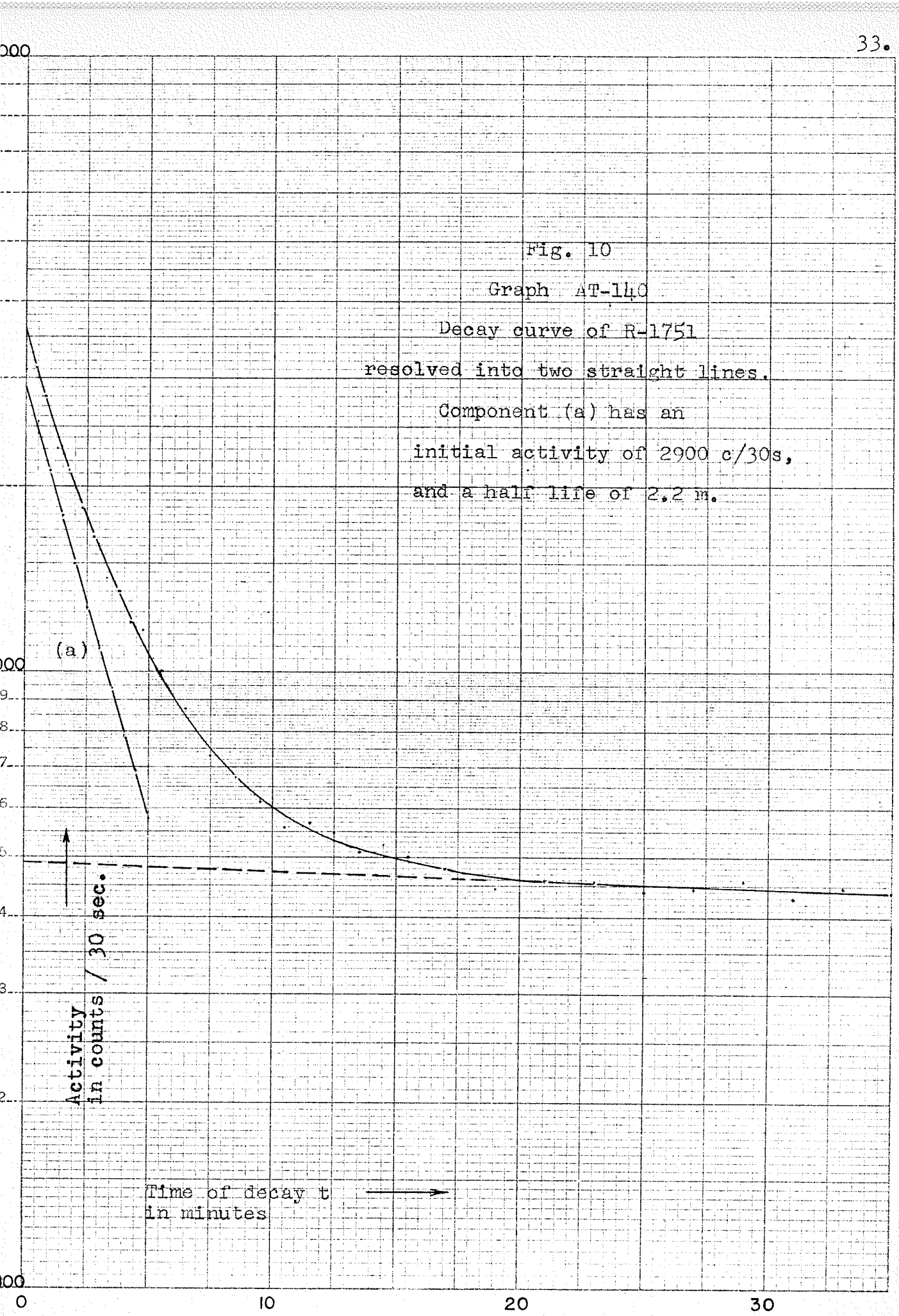

Fig. 10

Graph AT-140

Decay curve of R-1751 resolved into two straight lines. Component (a) has an initial activity of 2900 c/30s, and a half life of 2.2 m.

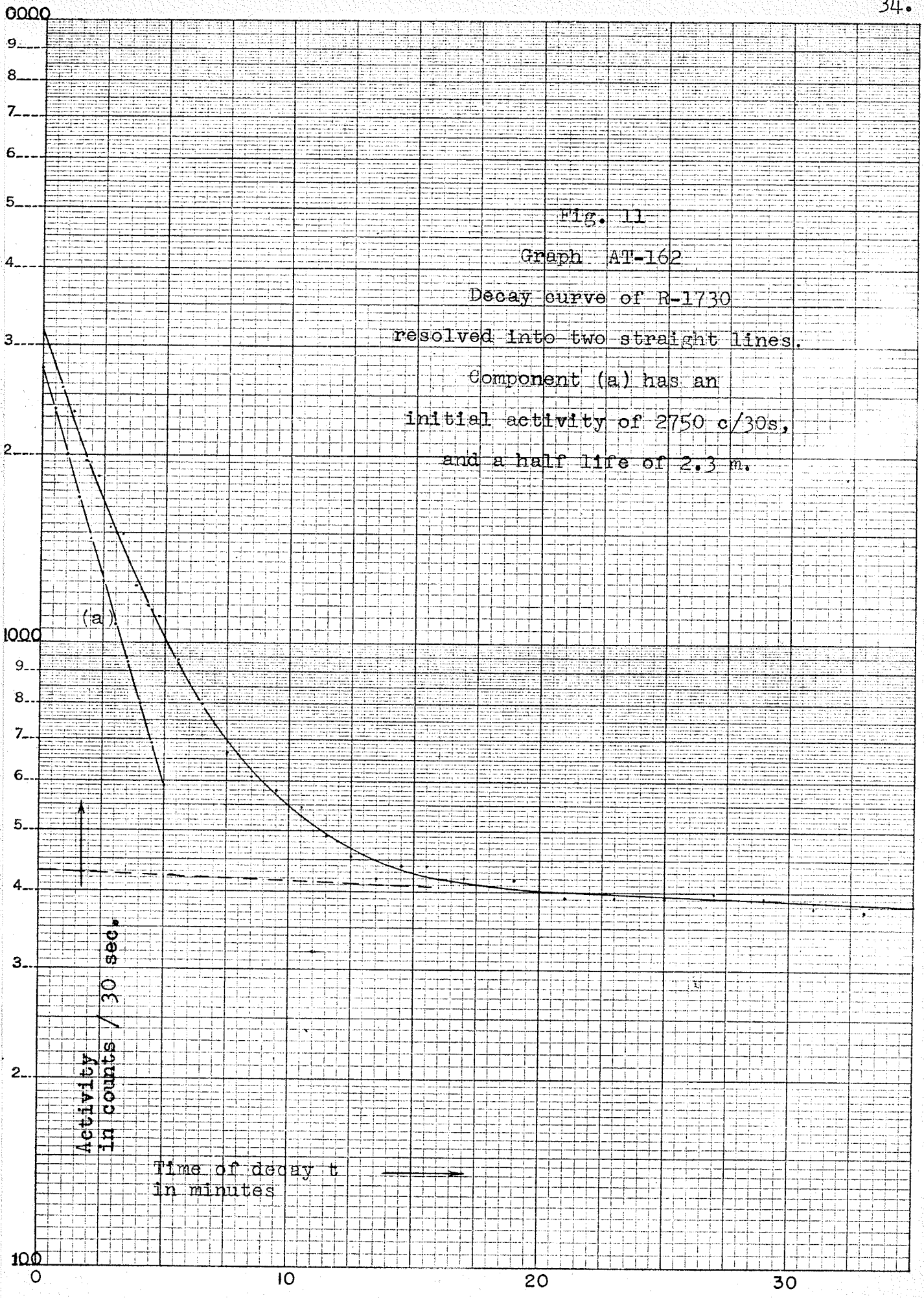

Fig. 11

Graph AT-162

Decay curve of R-1730 resolved into two straight lines. Component (a) has an initial activity of 2750 c/30s, and a half life of 2.3 m.

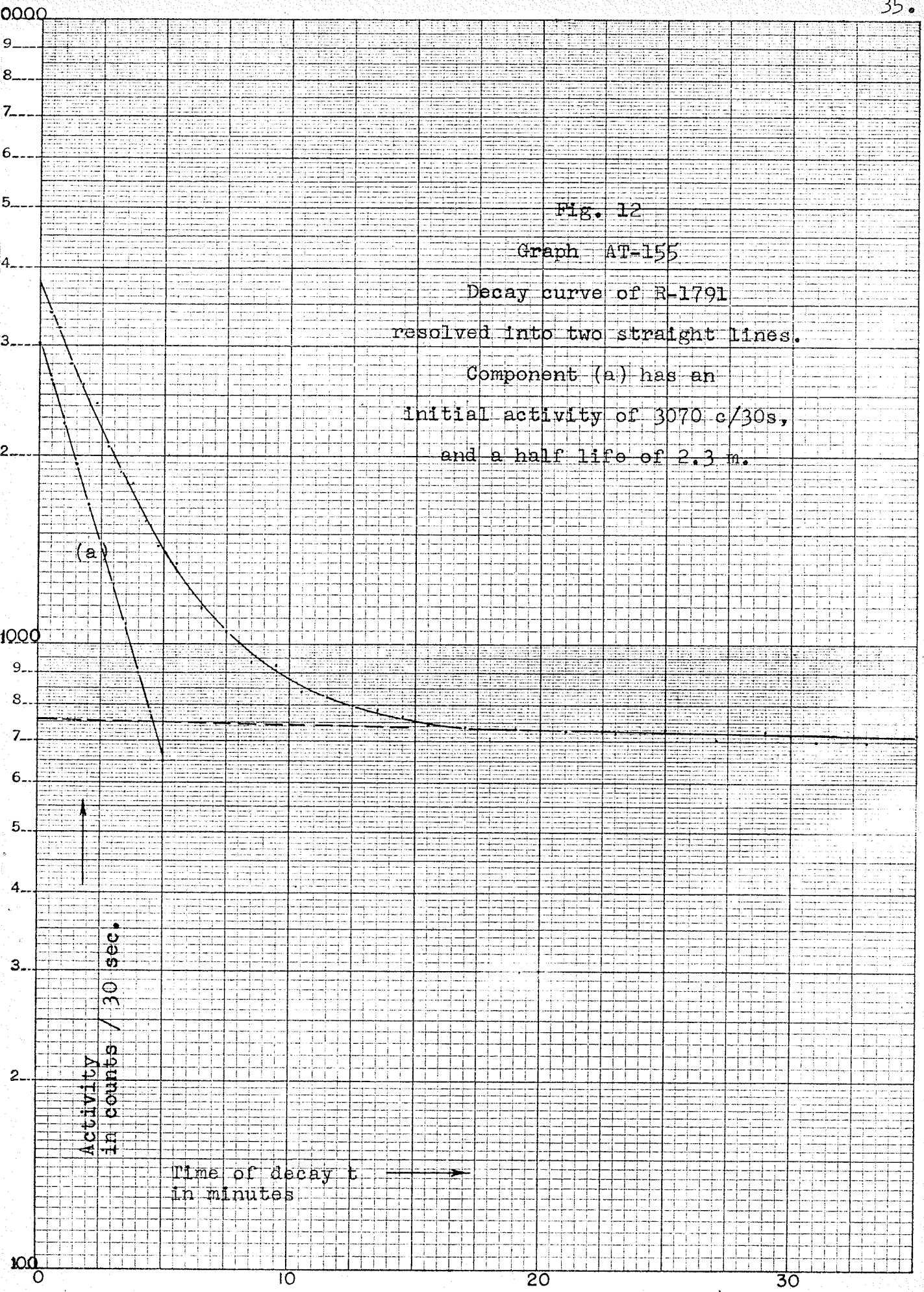

Fig. 12

Graph AT-155

Decay curve of R-1791

resolved into two straight lines.

Component (a) has an

initial activity of 3070 c/30s,

and a half life of 2.3 m.

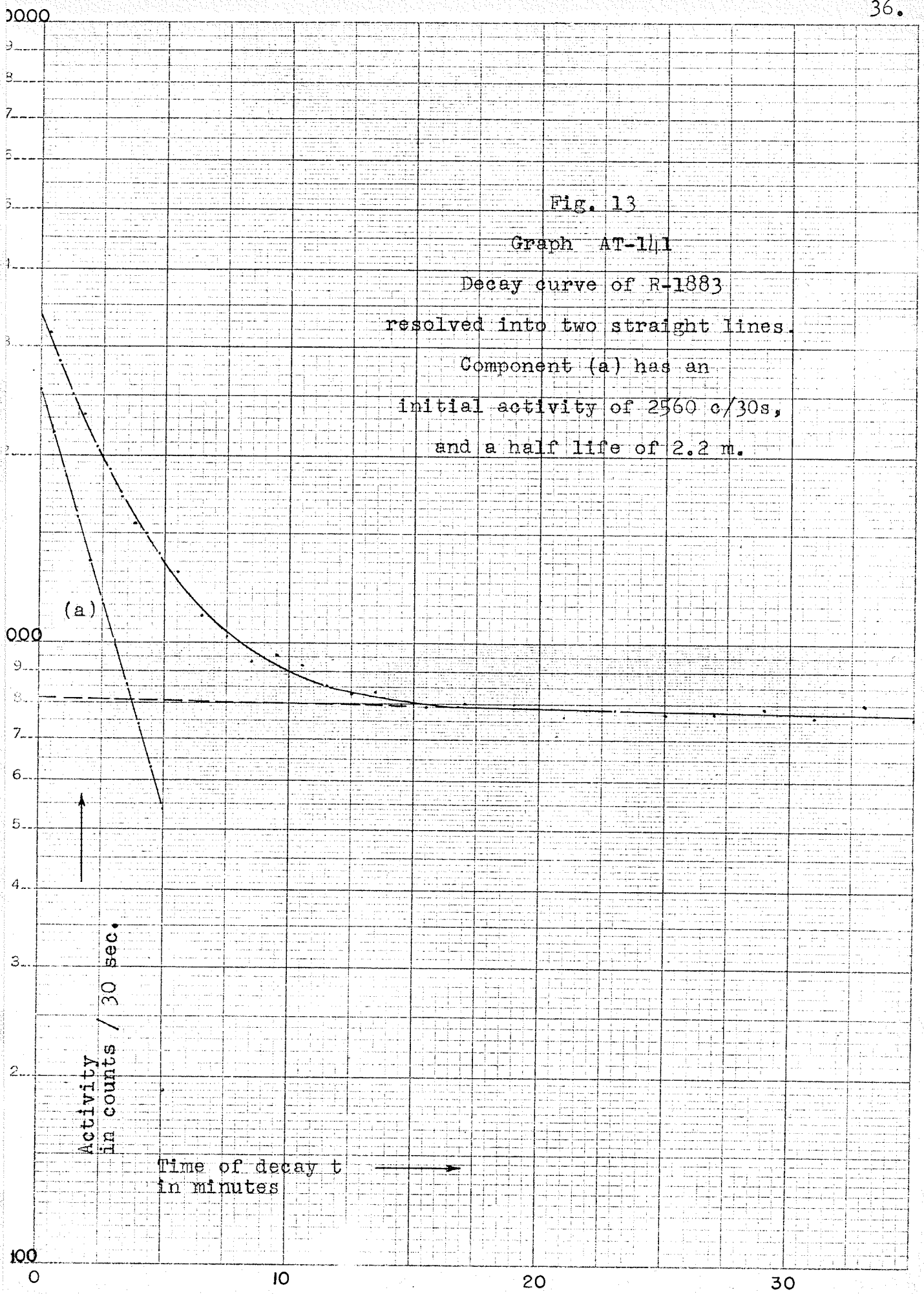

Fig. 13

Graph AT-1141

Decay curve of R-1883 resolved into two straight lines. Component (a) has an initial activity of 2560 c/30s, and a half life of 2.2 m.

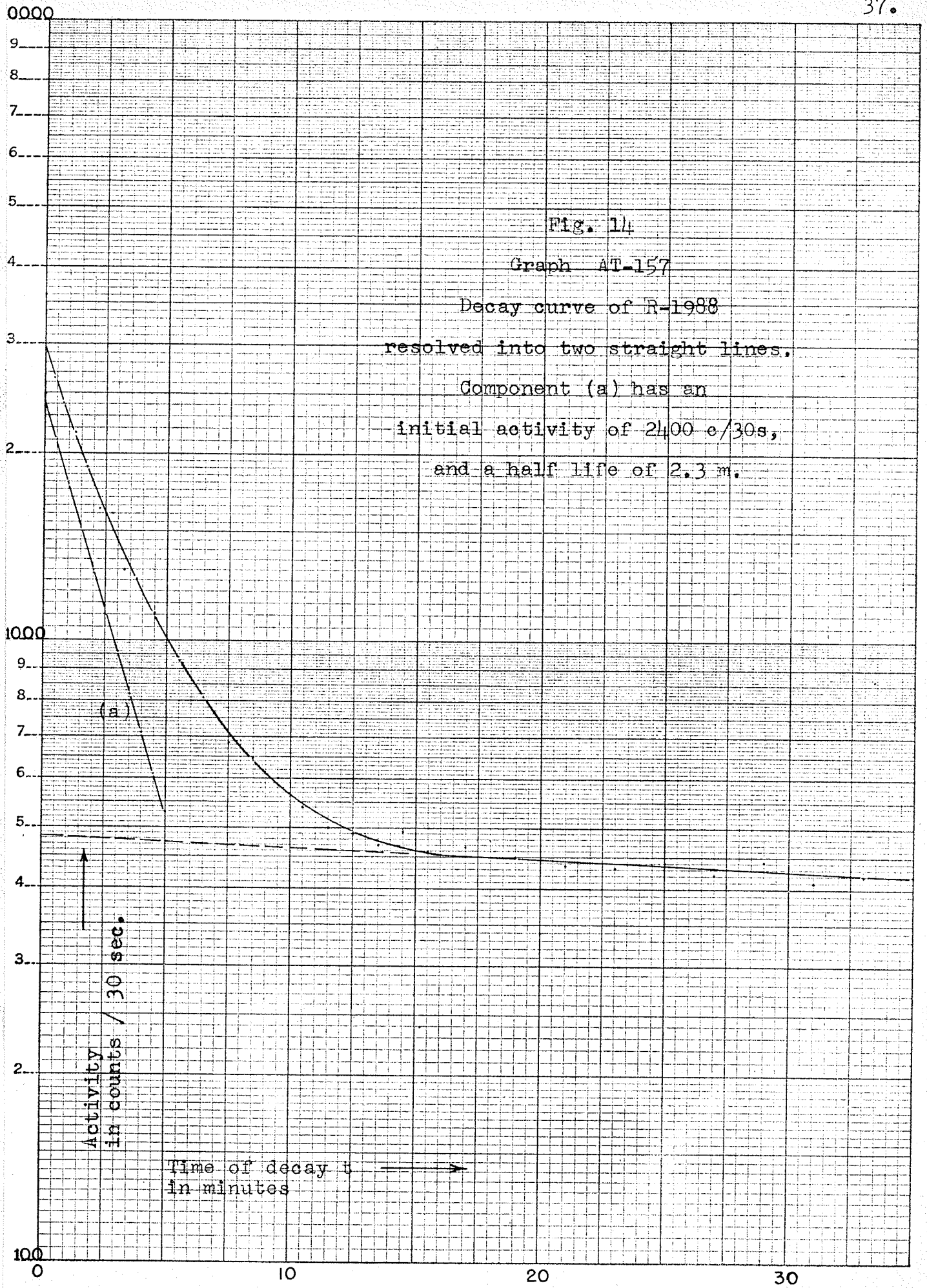

Fig. 14

Graph AT-157

Decay curve of R-1988

resolved into two straight lines.

Component (a) has an

initial activity of 2400 c/30s,

and a half life of 2.3 m.

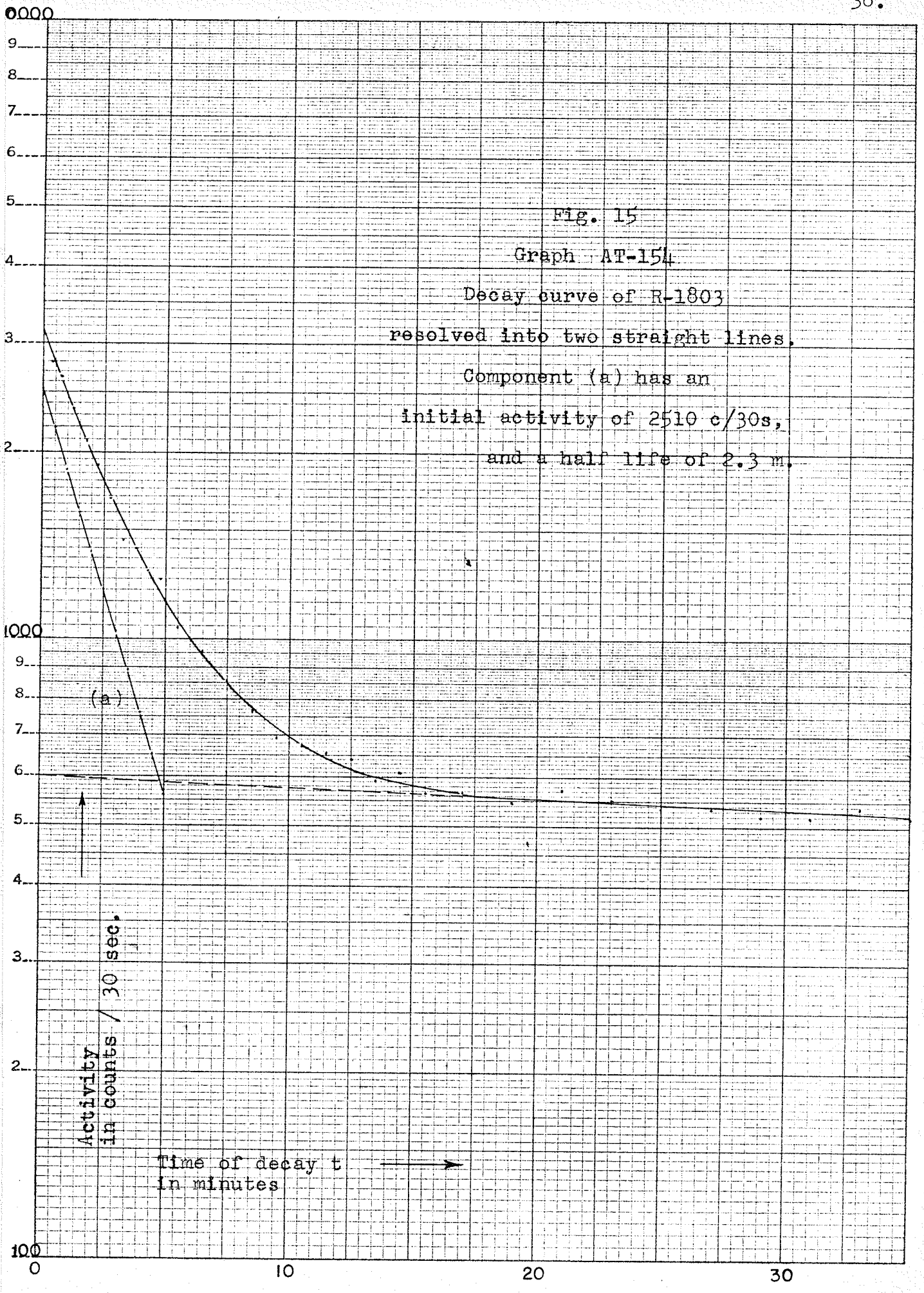

Fig. 15

Graph AT-154

Decay curve of R-1803

resolved into two straight lines.

Component (a) has an

initial activity of 2510 c/30s,

and a half life of 2.3 m.

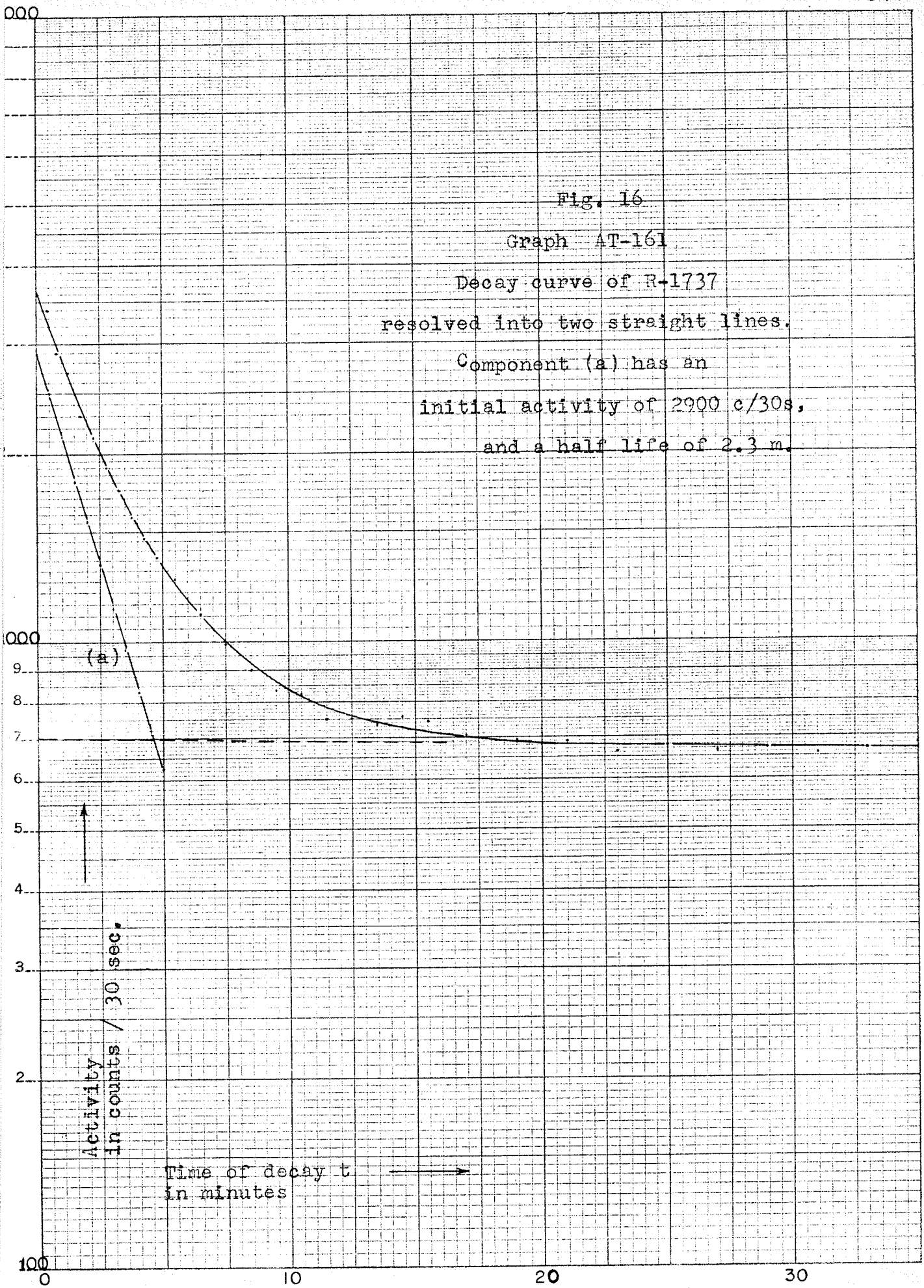

Fig. 16

Graph AT-161

Decay curve of R-1737 resolved into two straight lines. Component (a) has an initial activity of 2900 c/30s, and a half life of 2.3 m.

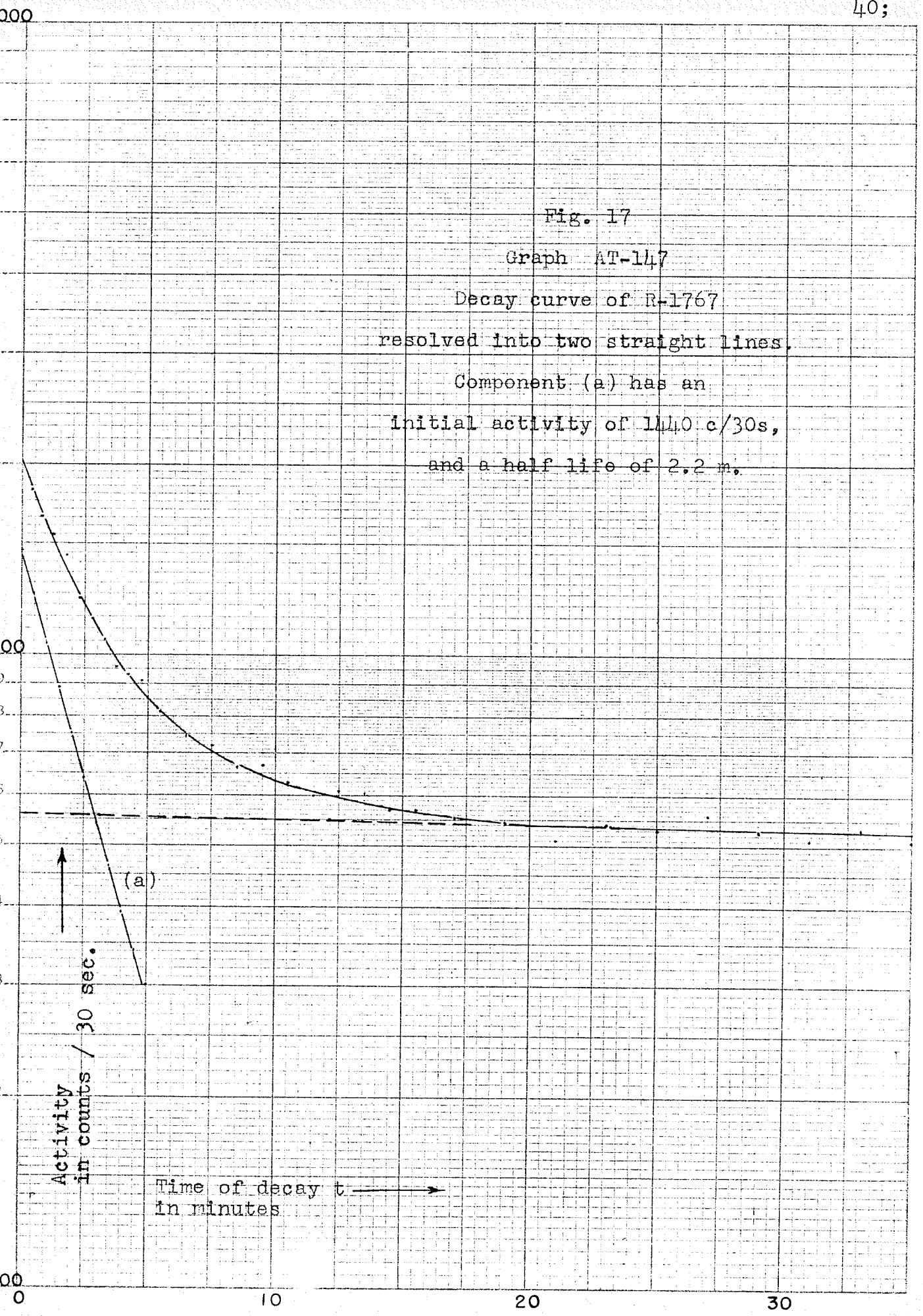

Fig. 17

Graph AT-147

Decay curve of R-1767

resolved into two straight lines.

Component (a) has an

initial activity of 1440 c/30s,

and a half life of 2.2 m.

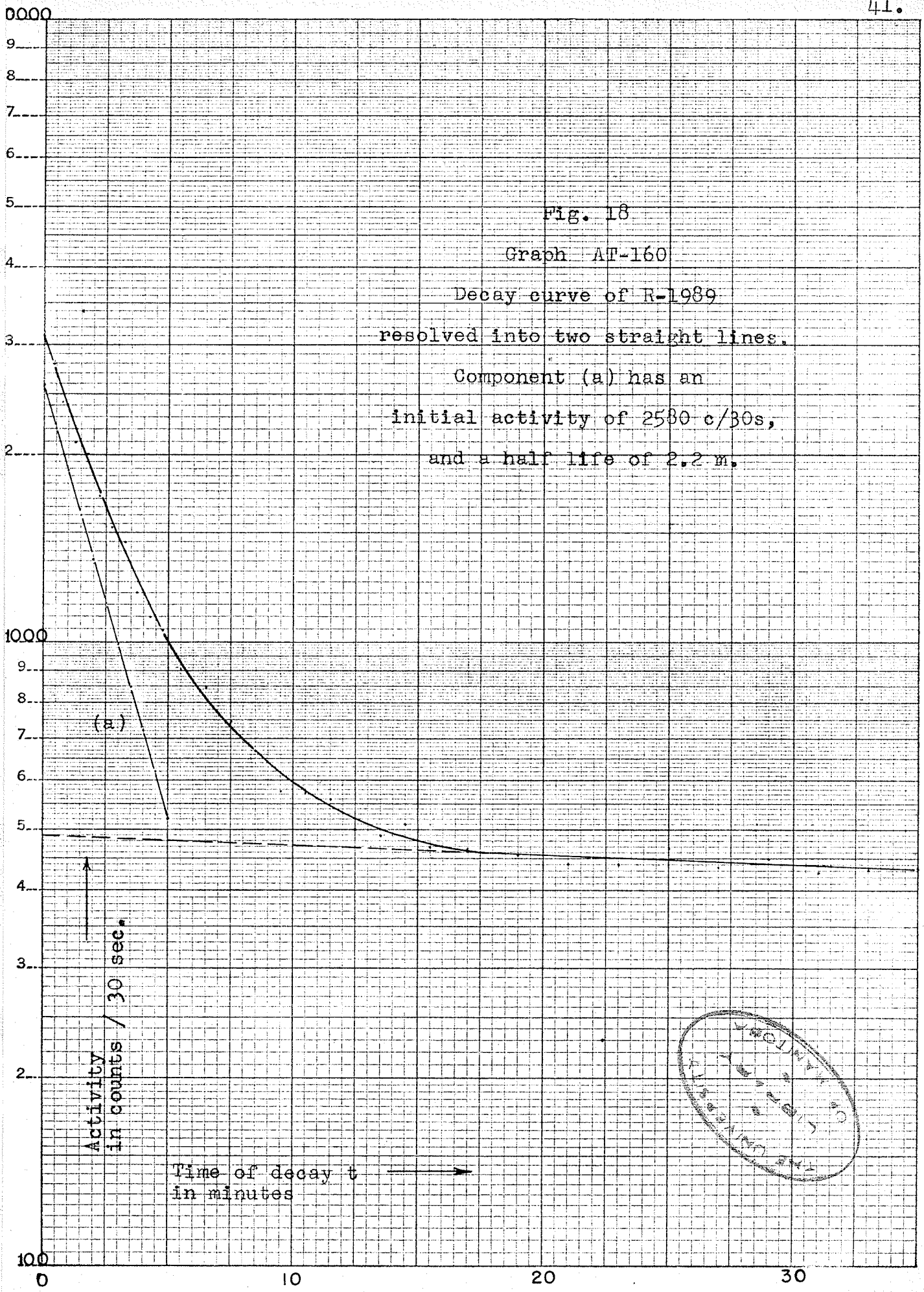

Fig. 18

Graph AT-160

Decay curve of R-1989

resolved into two straight lines.

Component (a) has an

initial activity of 2580 c/30s,

and a half life of 2.2 m.

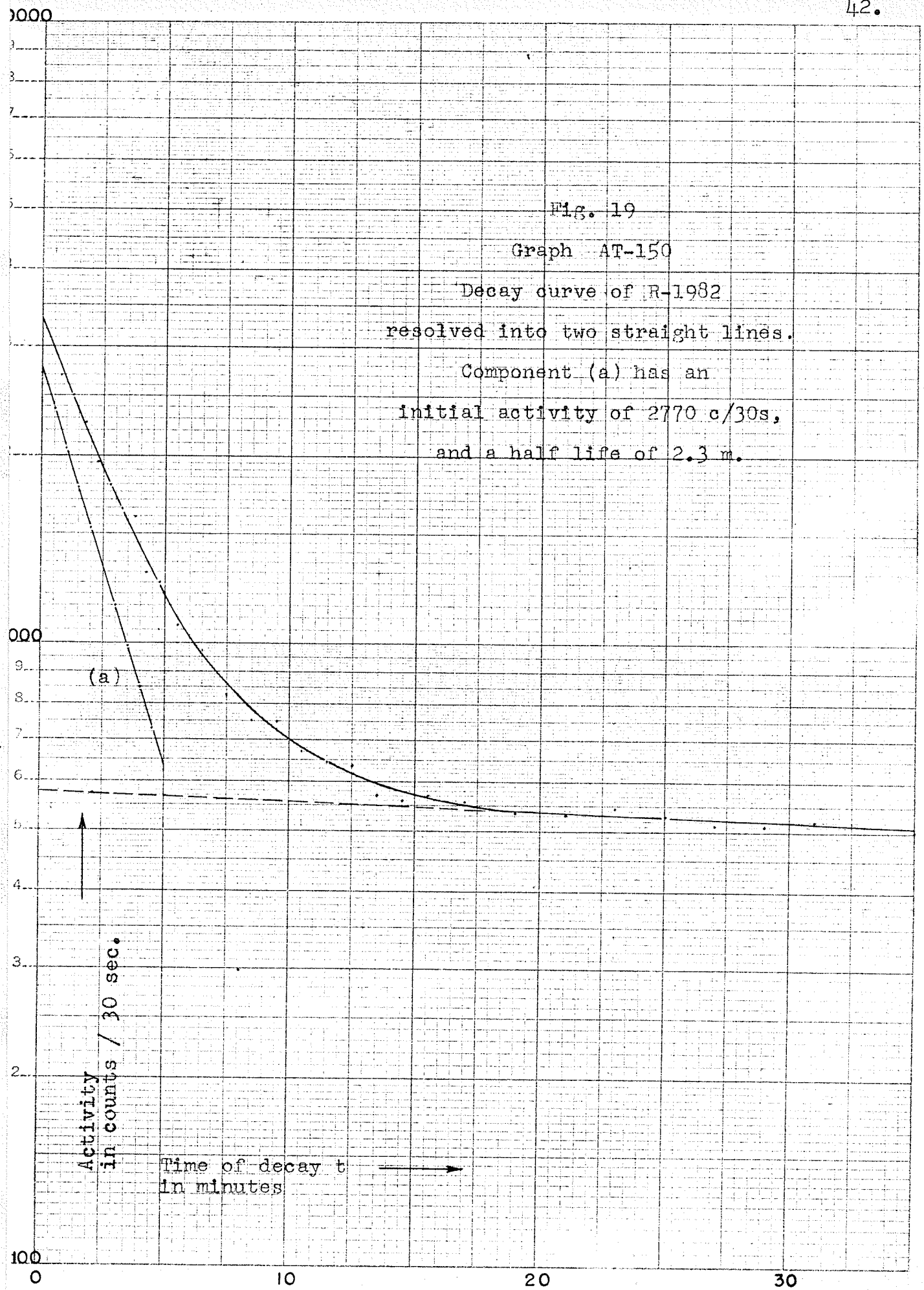

Fig. 19

Graph AT-150

Decay curve of R-1982

resolved into two straight lines.

Component (a) has an

initial activity of 2770 c/30s,

and a half life of 2.3 m.

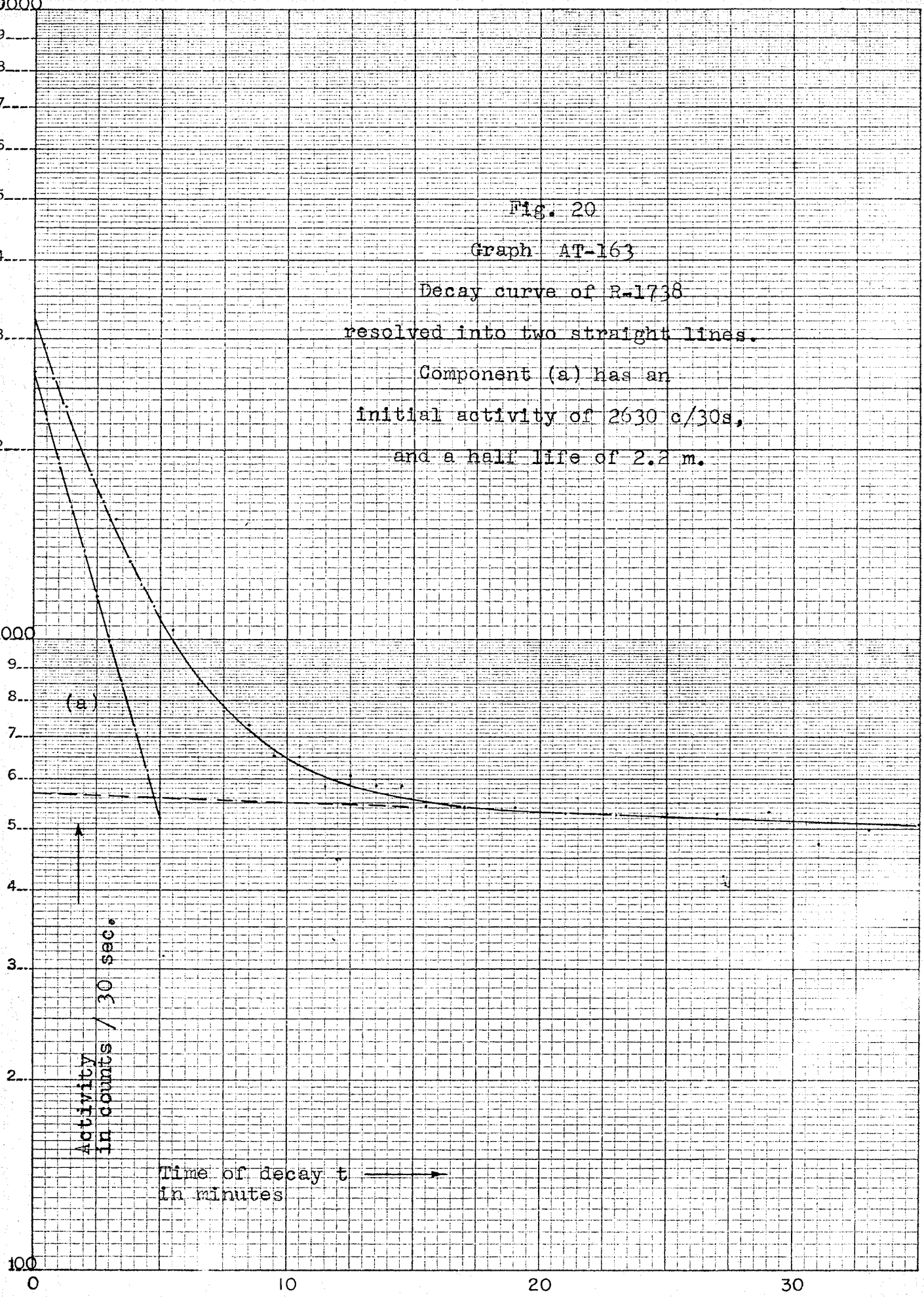

Fig. 20

Graph AT-163

Decay curve of R-1738 resolved into two straight lines. Component (a) has an initial activity of 2630 c/30s, and a half life of 2.2 m.

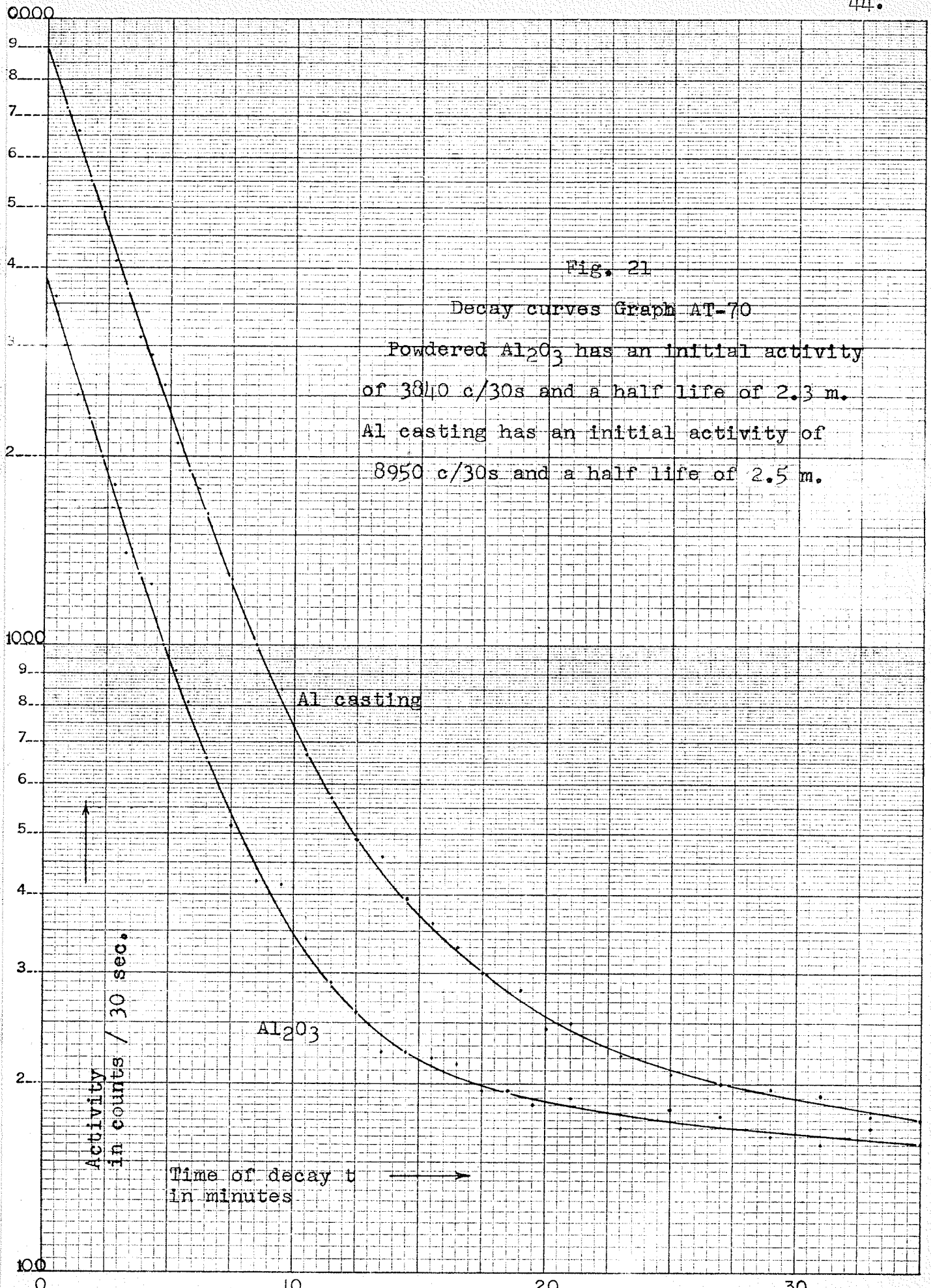

Fig. 21

Decay curves Graph AT-70

Powdered Al_2O_3 has an initial activity of 3840 c/30s and a half life of 2.3 m.

Al casting has an initial activity of 8950 c/30s and a half life of 2.5 m.

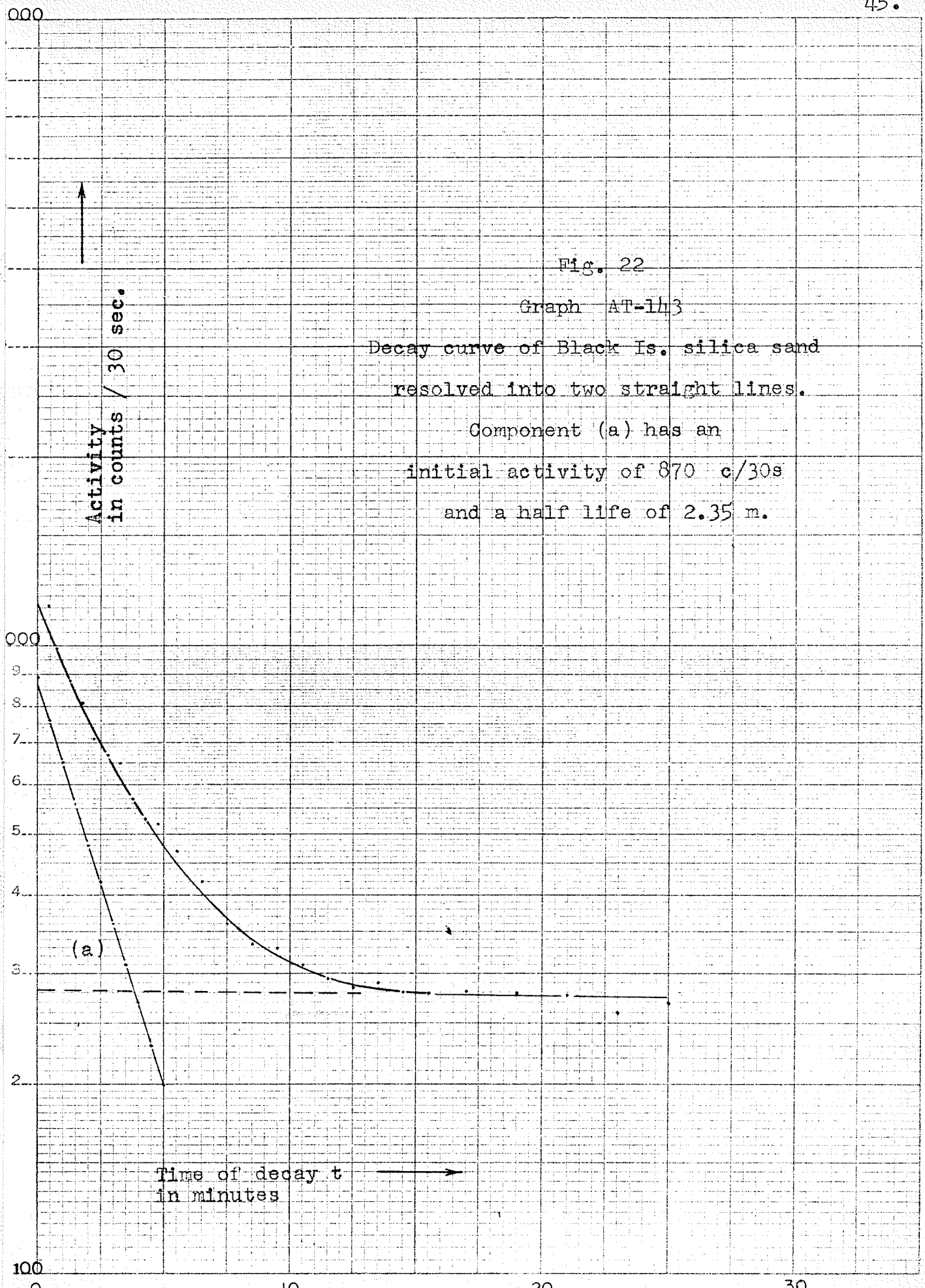

Fig. 22

Graph AT-1H3

Decay curve of Black Is. silica sand resolved into two straight lines. Component (a) has an initial activity of 870 c/30s and a half life of 2.35 m.

TABLE 3 EXPERIMENTAL DATA Al ANALYSIS IN IGNEOUS ROCKS

Date	Flux	Al Casting	Al_2O_3	1751	1730	1791	1883	1988	1803	1737	1767	1989	1982	1738
Sept. 29	10^2 *	19.3 *					18.7							19.8
Oct. 24	$7x10^3$	15.5					20.2							23.0
Nov. 1		24.0					21.2							26.1
Nov. 17			22.4				24.4							23.6
							27.0							24.7
Nov. 19							28.7							22.1
Nov. 25	$6x10^3$		13.8				13.5							10.5
							15.3							
Jan. 26	$5x10^4$	39.1				37.5								38.4
Jan. 28		38.9	31.5			37.9								38.8
							54.7							
Feb. 8							54.7							
Feb. 11							53.2			55.2				
							57.8			57.0				
Feb. 15	$4x10^4$													42.3
														41.8
Feb. 16														39.5
														40.5
Feb. 17							28.1			37.6				40.6
														40.8

* All values in C/30S/g Al_2O_3

‡ Approximate flux in $n/s/cm^2$

TABLE 3 (continued)

Date	Flux	Al Casting	Al_2O_3	1751	1730	1791	1883	1988	1803	1737	1767	1989	1982	1738
Feb. 18							39.4 39.4			41.1 41.1	42.9 43.7	41.9	45.3 44.3	47.7
Mar. 17				51.1			51.5			52.9				
Mar. 19		44.2	42.3	49.8			52.5 54.8			52.6	53.2	54.5 55.7		
Mar. 20				49.8			52.5 54.8 52.5			52.9	53.2 52.2	54.5 55.7	54.8	
Mar. 21						54.2 52.2		56.5 55.0	55.9		57.9	60.5	59.3	
Mar. 24					49.1	48.2		49.9	50.3		54.4	50.7	54.8	
Mar. 26					50.5		51.5				55.5	52.1		
Mar. 27	3.5×10^4			47.8	48.2	49.2	51.5	49.9	51.3	54.0	53.5	48.8	54.5	56.9

TABLE 3 (continued)

Date	Flux	Precision	Accuracy
Sept. 29	10^2		5.8
Oct. 24	$7x10^3$		13
Nov. 1			21
Nov. 17			3.5
Nov. 19		7.0 11.1	17.2
Nov. 25	$6x10^3$	12.8	36
Jan. 26	$5x10^4$		2.5
Jan. 28		1.1 0.5	2.4
Feb. 8		0.0	
Feb. 11		3.2 8.4	1.1
Feb. 15		1.2	
Feb. 16	$4x10^4$	2.5	
Feb. 17		0.5	
Feb. 18		0.0 0.0 1.6 2.2	1.9 3.4 3.4 4.2 5.2 6.2 6.7 8.8 9.5 13.5
Mar. 17			0.8 2.7 3.5

TABLE 3 (continued)

Date	Flux	Precision	Accuracy
Mar. 19		2.3 4.3	0.8 1.1 2.3 2.8 1.9 3.5 4.3 4.8 5.3 6.6 7.2 10.0
Mar. 20		0.0 1.9 2.2 4.3 4.3	0.4 0.6 0.8 1.1 2.8 3.3 3.6 4.1 4.3 4.5 5.7 6.1 6.8 9.6 10.1
Mar. 21		2.7 3.8	0.4 2.0 2.4 3.0 3.9 4.4 4.4 5.0 5.9 6.3 7.9 8.3 8.5 10.6 12.7
Mar. 24			0.8 0.8 0.8 1.6 1.6 1.8 2.4 3.2 3.4 4.2 4.9 7.5 7.8 7.9 8.8 8.8 9.5 10.2 11.0 12.3 13.2
Mar. 26			1.2 2.0 3.1 4.8 6.3 7.5
Mar. 27	3.5×10^4		0.4 0.8 0.8 0.9 0.9 1.2 1.4 1.4 1.9 2.0 2.0 3.8 2.2 2.8 3.2 3.4 3.4 4.2 4.2 4.2 4.4 4.6 4.8 5.0 5.1 5.3 5.4 5.6 6.1 6.2 6.2 6.6 7.0 7.0 7.4 8.0 8.4 8.8 9.2 9.3 10.1 10.2 10.2 10.3 10.5 11.0 11.2 11.3 12.2 13.0 13.1 14.8 15.2 16.6 17.3

3. Error. The sources of error were discussed on page 25, and in this section the amount of error found in the analysis of chemically analysed standards will be reported.

Precision. The error in the repetition of a standard in percent is showin in the second part of table 3. This data is plotted as a histogram in fig. 23. The shape of the histogram indicates that the error is distributed according to the Gaussian curve, that is, normal statistical distribution from zero. This is the distribution of compensating and statistical errors. The standard deviation is

$$\sigma = \sqrt{\frac{1}{n} \sum^{n} (\text{deviation})^2}$$

$$= 4.3\%$$

This means that the probability is 68.3% that the error of any repetition will be less than 4.3%.

Accuracy. If any of the standard samples was considered as an unknown, then the Al_2O_3 content would be found by dividing the corrected initial activity by the activation constant of another standard sample. The error, in relative percent, between the given and experimentally determined Al_2O_3 content will be, however, the same as that found by comparing the activation constants directly. Therefore, in table 3, the relative error between activation constants was calculated for every combination of determinations. These

errors are shown in the second part of table 3, and are plotted as a histogram in fig. 24. The shape of the histogram indicates a Gaussian distribution, but it is a broader curve than fig. 23 for the precision. The standard deviation is 6.95%.

The error would be considerably reduced if comparison was made only between similar rock types. Table 3 shows that the activation constant increases in the basic rocks, and this produces systematic error. In table 3, the rocks are listed in order of increasing activation content, and this is also the order syenite-granite-diorite-basic rock. R-1738 is the only anomaly.

The errors in the analysis of the acid rocks, R-1751, 1730, 1791, and 1883, considered separately, have a standard deviation of 6.24%. For the basic rocks 1988, 1803, 1767, 1989, and 1982, which make up most of the experimental data, the standard deviation is 5.42%. The error frequency histogram is shown in fig. 25.

It is reasonable to assume that most of the larger errors were caused by fluctuations in the equipment. It is known that the counter sensitivity is variable. These conditions can be improved. Therefore, the lowest standard deviation found can be confidantly used.

If the Si analysis had been done by this method (Knutson 1954), and was therefore subject to $\pm$ 2.5% error, the increased error of the Al analysis from the Si correction would be $\pm$ 0.52%.

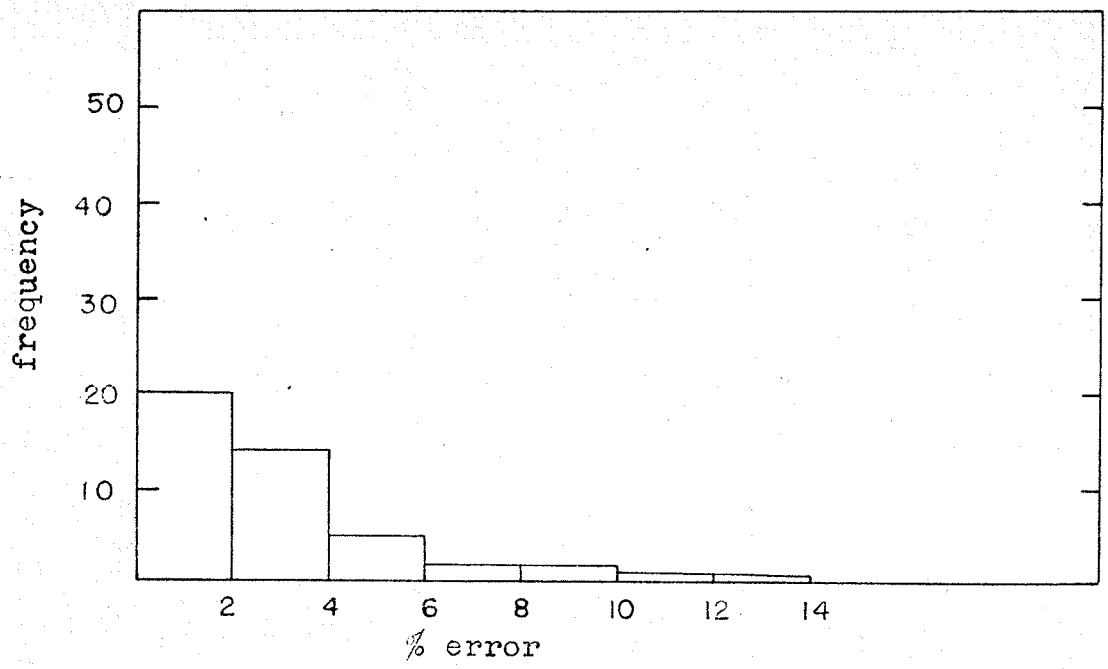

Fig.23 Precision of Al analysis in igneous rocks

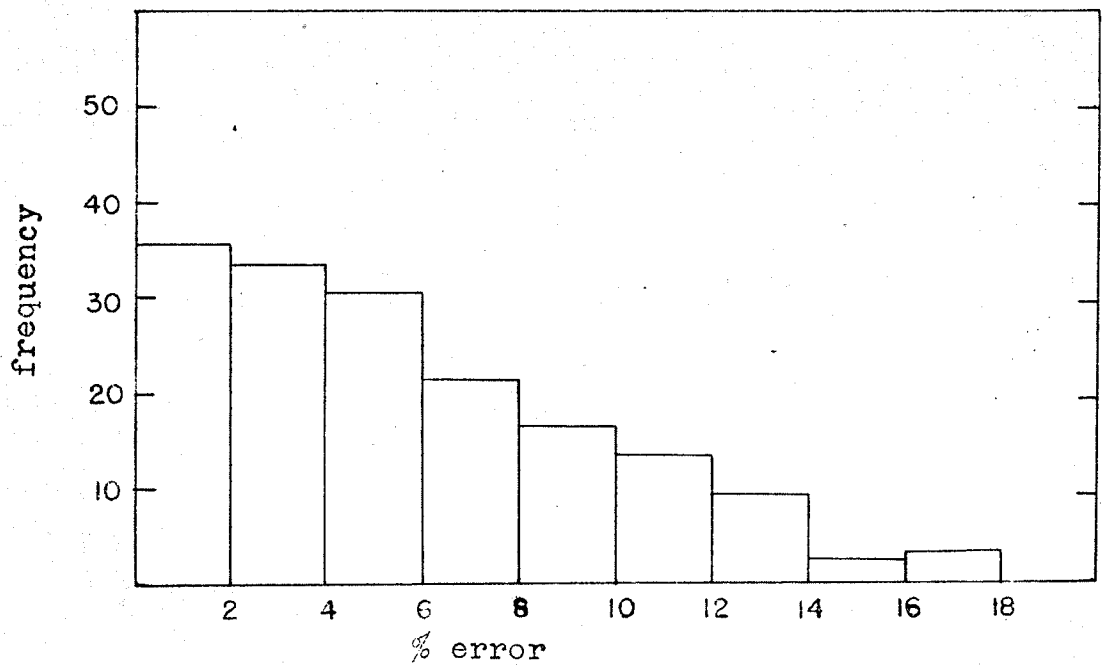

Fig.24 Accuracy of Al analysis in igneous rocks

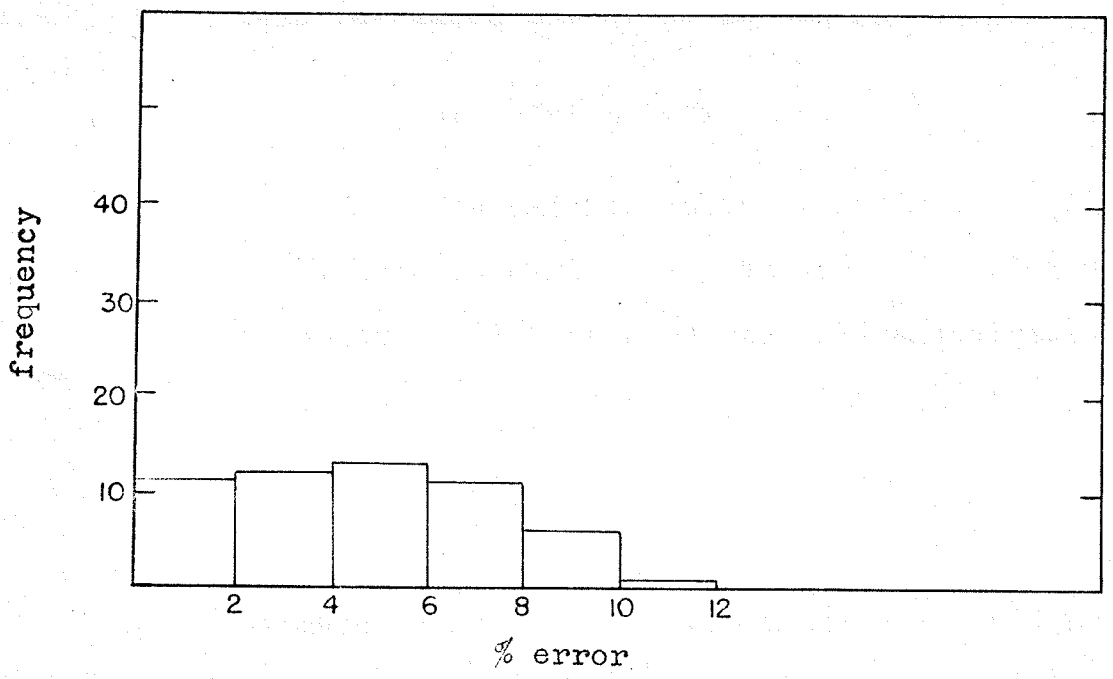

Fig. 25 Accuracy of Al analysis in basic igneous rocks

This increases the error in the Al analysis to ± 5.94%.

4. Conclusions

The induced activity analysis of Al in an igneous rock, when compared to a standard of a similar type, and allowing ± 2.5% error in the silica analysis, will have a probable error within 6%, and may therefore be reported as 15 ± 0.9% Al_2O_3.

Starting with crushed samples, 9 determinations can be made in an 8 hour day, of which 3 would be standards, 6 unknowns. If the decay curves were recorded automatically, leaving the operator free for weighing and calculating, 12 determinations could be made. Therefore, the method is fast and suitable for routine work.

The decay curve of the Al casting does not have the same shape as the other samples, therefore its constant cannot be expected to be the same. It decays with a half life of 2.5 m, instead of 2.3 m., because of the impurities Cu, Mn, Ga, Zn, Co, and Sc in cast Al. Cu may be an 8% alloy; it has a half life of 4.34 m.; it is the probable cause of the longer half life.

The increase of the activation constant in the basic rocks may have two contributing causes. Firstly, the basic rocks are denser than the acid rocks, and because in most cases an equal weight sample, 300 g, was used, there was a slight difference in sample shape. The extra volume of the

lighter acid rocks fills the upper central part of the container, the part farthest from the neutron source and the surrounding oil bath that thermalizes the neutrons. It will be experimentally proven in the following section ''Al Analysis In Bauxites'' that the decrease in the activation constant by increasing the sample size is considerable. Secondly, the basic rocks have more activity caused by Fe and Mg, which may not be completely corrected for in the resolution of the 2.3 minute Al^{28} component.

ALUMINUM ANALYSIS IN BAUXITES

1. A set of 5 analysed samples of bauxite was kindly supplied by the Aluminum Laboratories Limited, Arvida, Quebec. The other bauxite was one used by Bramadat, and analysed by the Mines Branch, Winnipeg, (see table 4). On the 14th of April, 1956, Bauxites no. 2 and no. 5 were dehydrated over a meeker burner. There was some dust loss due to boiling of the powder. Some absorption of moisture from the air was noticed. The weight loss is therefore not accurately known, though complete dehydration was approached. The given analyses did not include H_2O and this was assumed to be the unaccounted for part of 100%. On this basis the analyses were recalculated to 100% and are included in table 4 as 2D and 4D (dehydrated). Except for Bramadat's bauxite, these samples are powder fine, and when loaded into the container they tend to fluff up, especially no.'s 4 and 5. The error caused by trying to reproduce the packing is

considered in section 3, below

2. Experimental data. The decay curves for the activated bauxites are shown in figures 27 to 32. The activation constants, in c/30s/g Al_2O_3, obtained from these curves, are given in table 6.

3. Error. The experimentally determined error is shown in the second part of table 6, calculated from the comparison of the separate determinations. Sources of error are the same as in igneous rocks and are given theoretical consideration on page 25.

It was experimentally difficult to fill the containers to the same level every time, because of the fluffy nature of the bauxite powders, and this is believed to be the major source of experimental error. The seriousness of changes in sample shape and size was tested by running different weights of a sample. The data of these experiments is shown in table 5. Fig. 26 presents the results graphically, and shows the pronounced decrease in the induced activity as the containers are filled with larger amounts of the sample. An estimated weight variation in the actual experiments is 20 g; this would cause an error of about 8%, and accounts for the poor results of bauxite determinations.

Precision. The precision in repetition is shown in table 6, and is plotted as a histogram in fig. 33. The standard deviation is smaller than that of the igneous rocks although

TABLE 4 ANALYSES OF BAUXITE SAMPLES

	Bramadat's Bauxite	1	2	2D	3	4	4D	5
Al_2O_3	55.47	51.33	53.18	72.8	60.52	49.73	70.0	46.14
SiO_2		4.10	0.81	1.11	4.43	0.36	0.51	3.87
Fe_2O_3	6.01	15.34	12.08	16.52	1.78	18.38	25.9	18.82
TiO_2	0.27	1.44	2.46	3.37	2.60	2.50	3.52	2.12

TABLE 5

EFFECT OF CHANGE OF SAMPLE SIZE ON BAUXITE DETERMINATIONS

sample	sample weight	sample shape	weight Al_2O_3	initial activity	c/30s/g Al_2O_3
4D	100g	fig. 26 A	70	3200	45.6
4D	130		91	3780	41.5
4D	170		119	4300	36.1
4D	210	fig. 26 B	147	4550	30.1
5	100	fig. 26 A	46.14	2600	56.3
5	120		55.4	2960	53.4
5	160		73.9	3450	46.6
5	210	fig. 26 B	97.0	3860	39.8

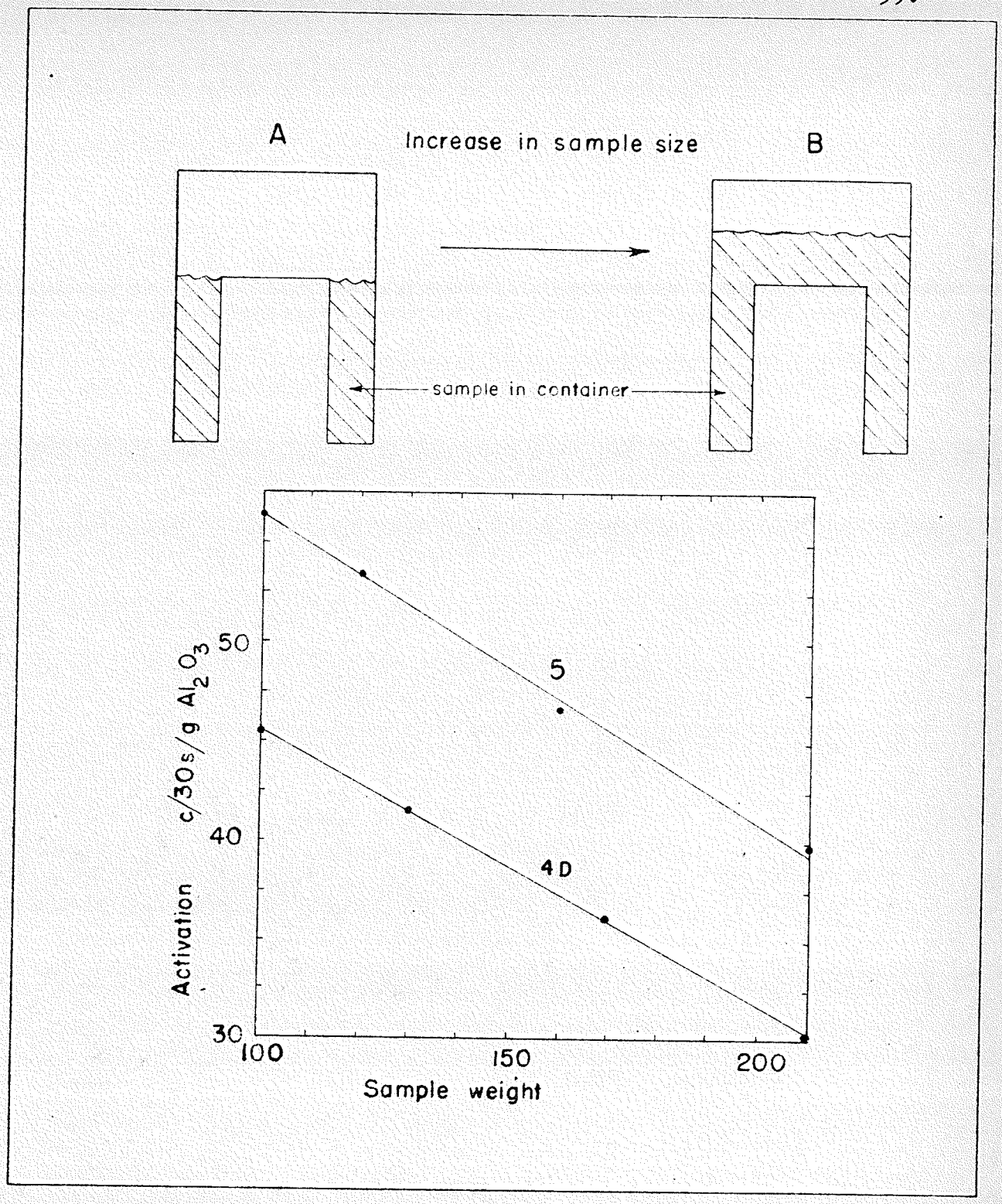

Fig. 26 Effect of change of sample size on bauxite determinations

they should theoretically be the same. The discrepancy is probably due to the small number of repeat experiments done on the bauxites, and to the fact that many of these were repeated without changing the sample, thereby eliminating weighing and packing errors.

Accuracy. The error between each combination of determinations is shown in table 6. Fig. 34 is a histogram of the error frequency. The histograms illustrate the discrepancy between the precision and accuracy of Al analysis in bauxites, and show large experimental errors. In general, the fluffy bauxites no.'s 4 and 5 gave lower activation constants than the others. Although fig. 34 does not suggest a Gaussian curve, the standard deviation is 11.7% for comparison with the other standard deviations.

4. Conclusions.

Induced activity analysis in bauxites was not performed satisfactorily. Although theoretically feasible, the experimental determinations gave high errors. The probable source of these large errors is in packing. Better results would be obtained by using a volumetric container and a coarser sample, say plus 40 mesh.

In the containers used, the induced activity is not evenly distributed. The part in the bottom, between the two cylinder walls (see fig. 8), is closer to the neutron source and the surrounding oil bath that thermalizes the neutrons,

and this part of the sample contributes the main part of the induced activity. Also, the increased gamma absorption in the top part of the sample as it gets thicker would add to this effect. Little is gained if the sample size is increased by piling up on top.

The bauxite samples contained less than 5% silica, and the correction was negligible.

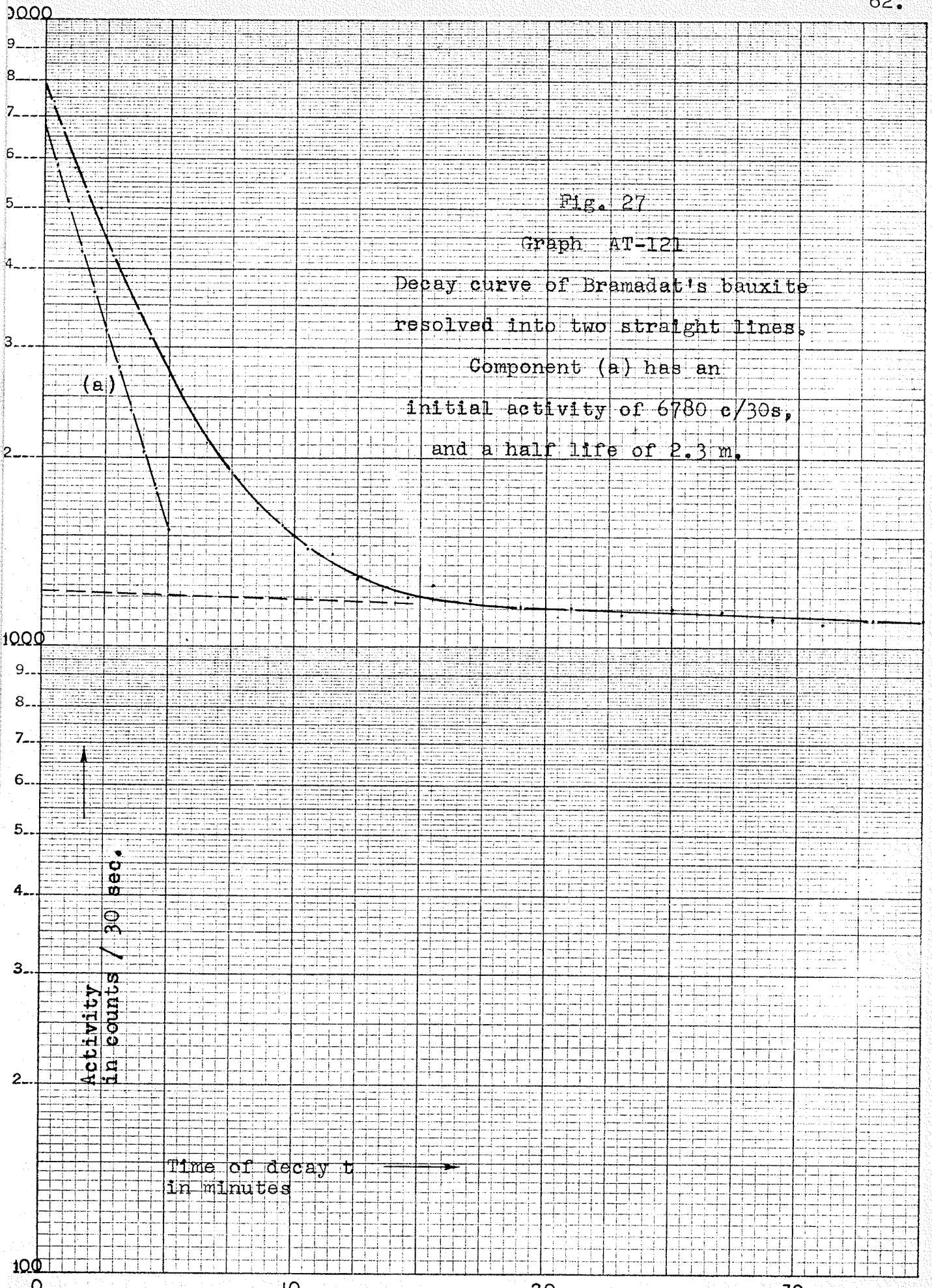

Fig. 27

Graph AT-121

Decay curve of Bramadat's bauxite resolved into two straight lines. Component (a) has an initial activity of 6780 c/30s, and a half life of 2.3 m.

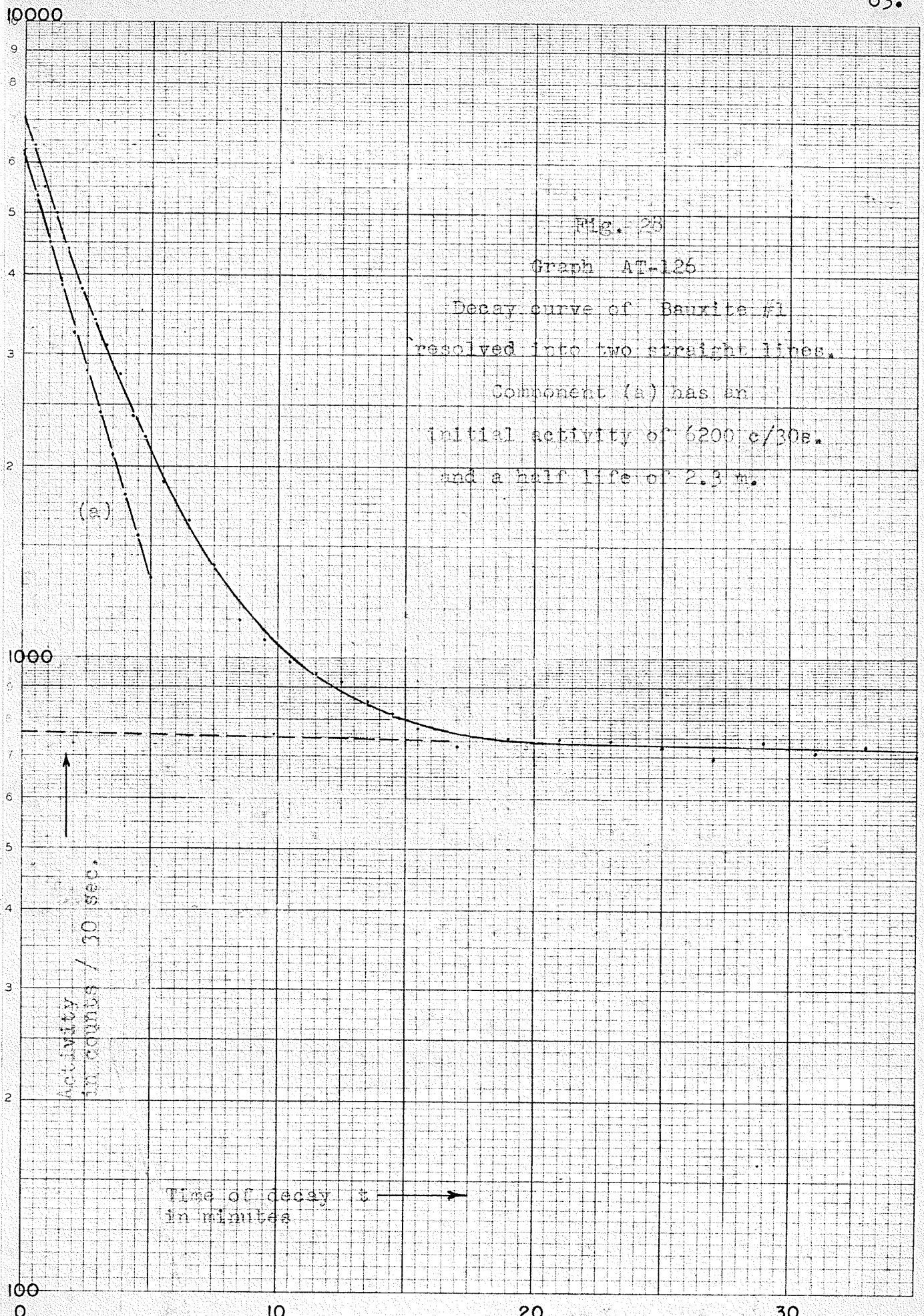

Fig. 25

Graph AT-125

Decay curve of Bauxite #1 resolved into two straight lines. Component (a) has an initial activity of 6200 c/30s. and a half life of 2.3 m.

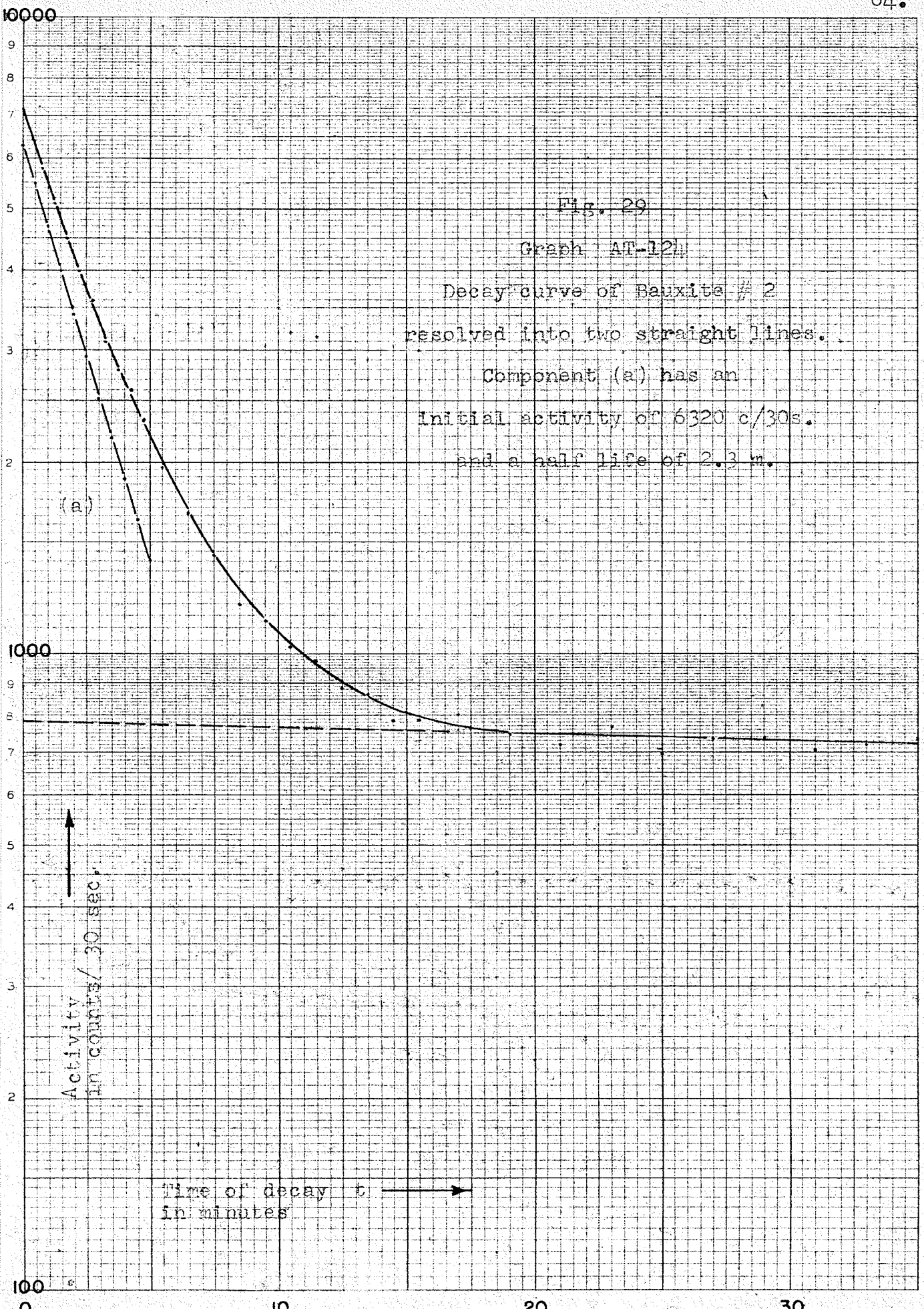

Fig. 29

Graph AT-124

Decay Curve of Bauxite # 2 resolved into two straight lines. Component (a) has an Initial activity of 6320 c/30s. and a half life of 2.3 m.

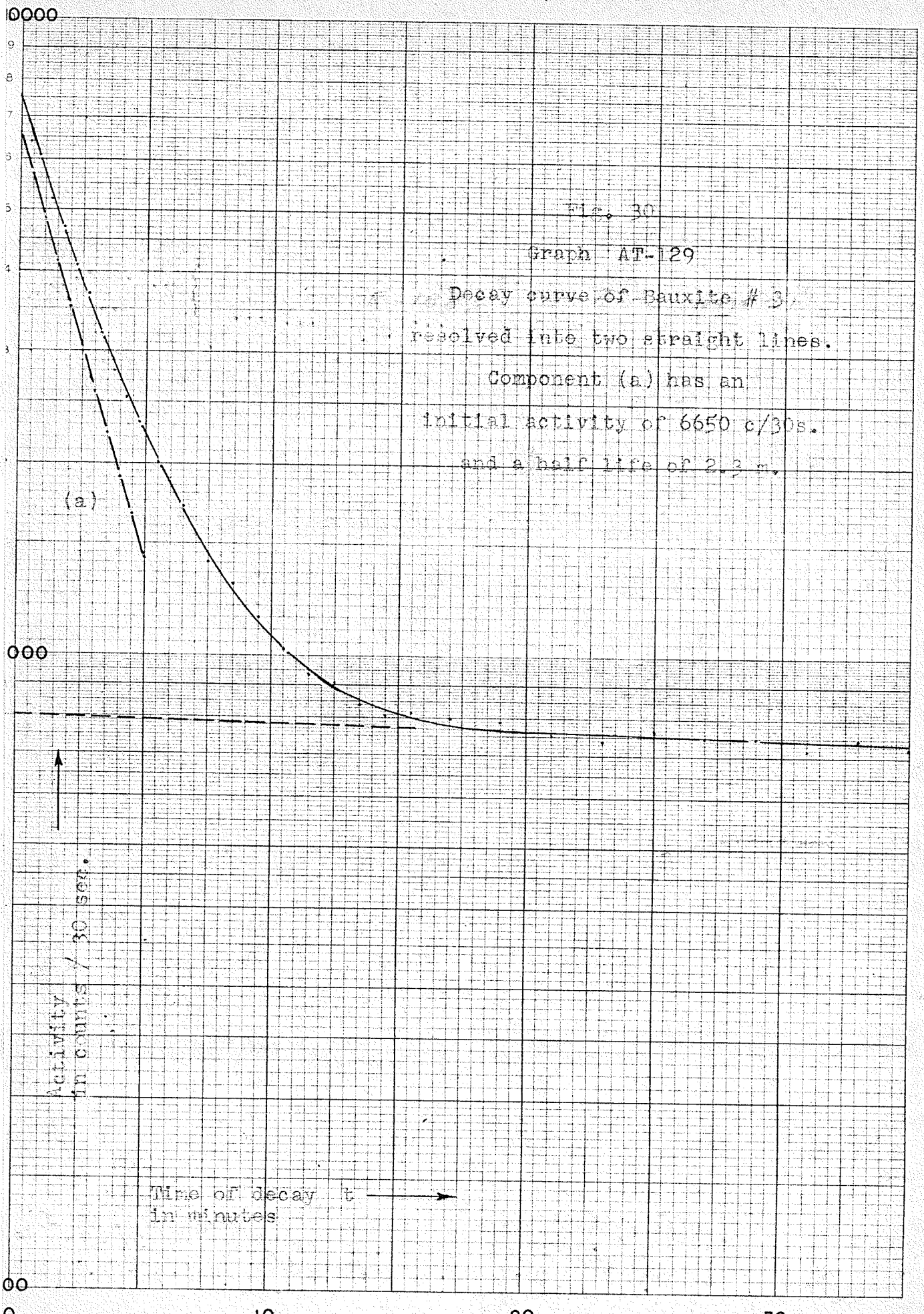

Fig. 30

Graph AT-129

Decay curve of Bauxite # 3 resolved into two straight lines. Component (a) has an initial activity of 6650 c/30s. and a half life of 2.3 m.

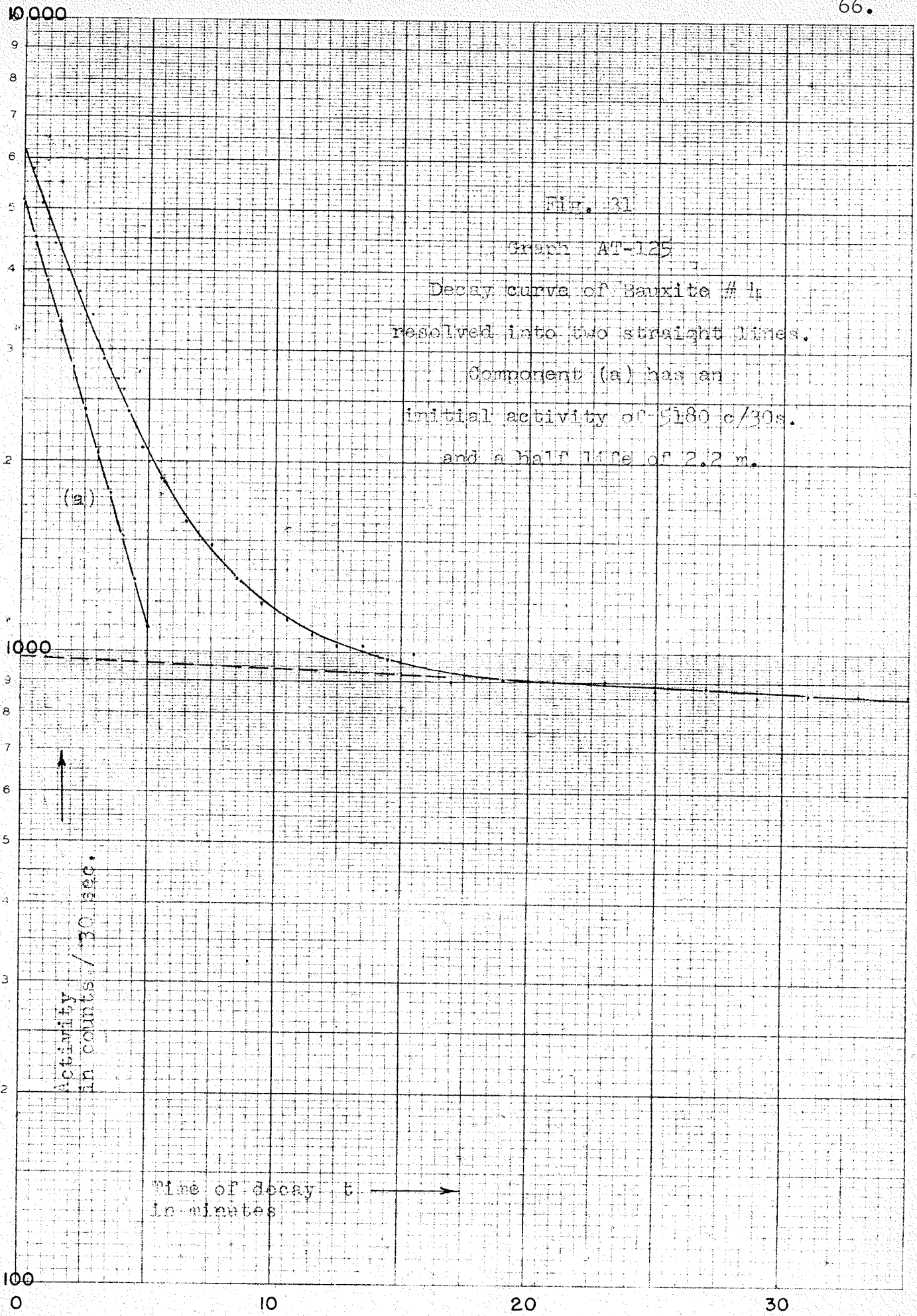

Fig. 31

Graph AT-125

Decay curve of Bauxite # 4

resolved into two straight lines.

Component (a) has an

initial activity of 5180 c/30s.

and a half life of 2.2 m.

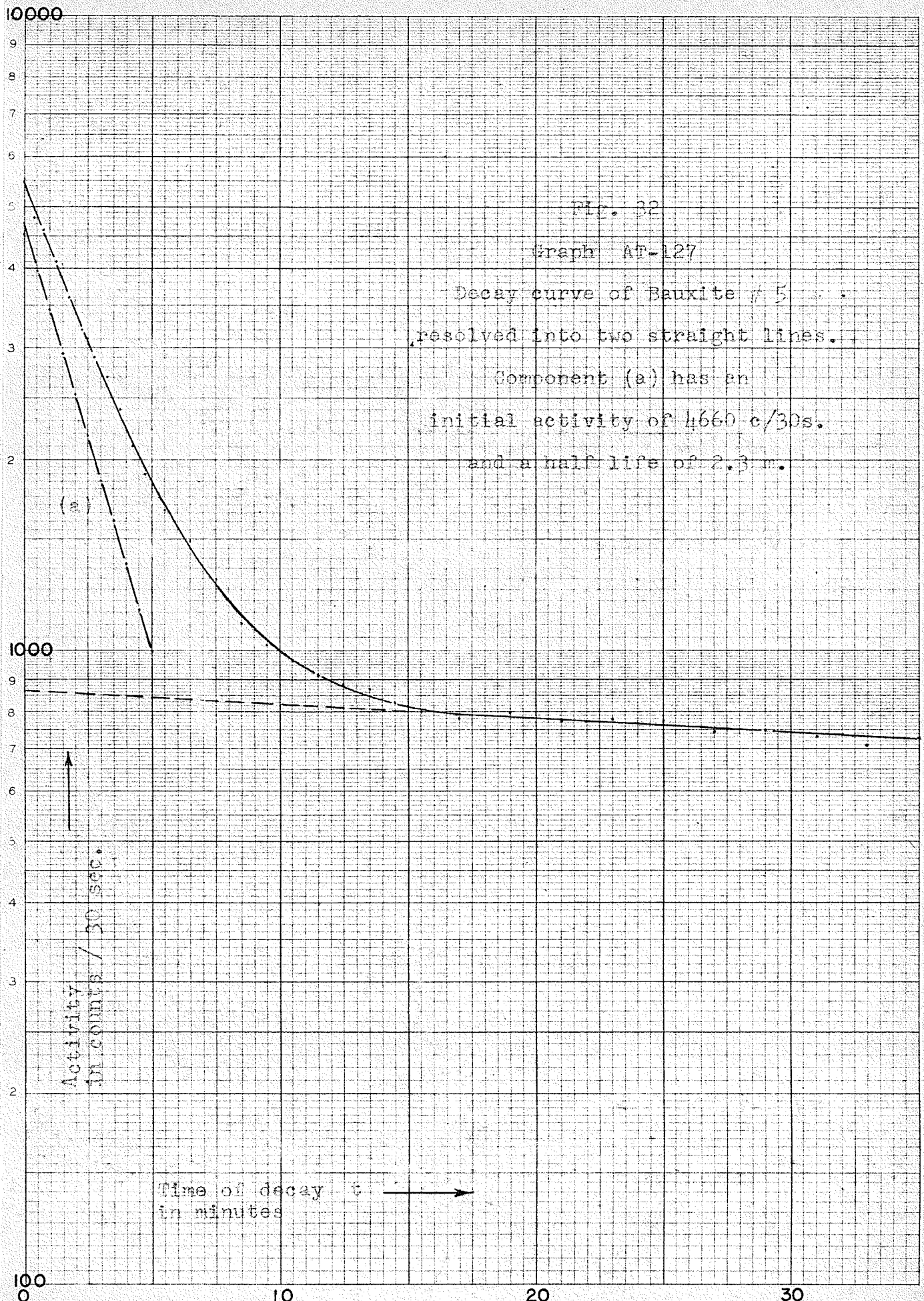

Fig. 32

Graph AF-127

Decay curve of Bauxite # 5 resolved into two straight lines. Component (a) has an initial activity of 4660 c/30s. and a half life of 2.3 m.

TABLE 6 EXPERIMENTAL DATA Al ANALYSIS IN BAUXITES

Date	Flux	Al Casting	Al_2O_3	Bramadat's Bauxite	No.1	No.2	No.3	No.4	No.5	Precision	Accuracy
Dec.1	$6x10^3$		12.8 13.0	11.0 11.0						1.5 0.0	16.0
Dec.2	$6x10^3$		12.6 12.2	11.1 11.2						0.9 3.2	10.6
Jan.26	$5x10^4$		39.1	32.4							
Feb.1						55.0 55.0 51.2	52.1 52.8	40.6 40.6	39.4 42.0	0.0 0.0 1.3 7.1 7.1 6.5	2.5 2.5 29 29 25 25
Feb.19	$4x10^4$			41.9	37.3 38.1	38.5 39.4	38.6	34.7 34.7	36.8 36.8	0.0 0.0 2.1 2.2	1.0 2.2 2.4 3.4 5.8 5.9 8.3 10.7 12.0 4.8
Mar.3		16.5		12.9	11.9		15.5				8.2 18.2 25
Mar.6		18.9		28.5 28.5	21.2 24.8		27.7 28.0			0.0 1.1 15.5	2.1 19.2 21.4
Mar.8		35.2		48.7 49.0	43.4 44.2		46.9 46.9	41.2		0.0 0.6 1.8	4.0 6.1 6.8 10.8 12.9 16.9

TABLE 6 (continued)

Date	Flux	Al Casting	Al_2O_3	Bramadat's Bauxite	No.1	No.2	No.3	No.4	No.5	Precision	Accuracy
Mar.10					48.1	47.5	43.8	41.6	40.2	0.0 0.0	0.6 3.4 5.2
					48.1	48.2		41.6		1.5	8.6 8.7 9.3
											13.9 14.5 17.3
											17.9
Mar.12				48.0	47.3	48.4	41.0	40.3	41.2		0.4 0.8 1.5
											2.3 1.7 2.2
											13.8 14.3 15.2
											15.7 16.0 17.5
											16.1 16.6 18.3
Mar.13				48.0	49.7	42.1	43.8	40.3	41.5		1.4 2.9 3.5
											4.0 4.3 5.4
											8.3 9.2 12.6
											13.1 16.5 17.4
											18.0 20.8
Mar.14				41.4	45.0	42.5	44.4	36.7	40.9	0.8 1.8	1.4 2.0 3.8
				46.0	45.8	39.8	41.8	35.4	39.8	2.7 3.6	4.7 5.2 6.1
								35.1		4.5 6.0	6.8 8.1 10.0
										6.6 10.5	11.9 12.1 14.1
											18.8 20.1 24.0
Apr.10		42.7	44.2	42.6	44.9	48.6	46.7	41.4	45.8		0.2 1.6 2.0
											2.0 2.9 3.1
											3.4 3.5 3.7
											3.9 4.0 5.0
											5.3 5.5 5.9
											6.5 7.0 7.2
											7.9 8.1 8.9
											9.2 9.5 10.1

TABLE 6 (continued)

Date	Flux	Al Casting	Al_2O_3	Bramadat's Bauxite	No.1	No.2	No.3	No.4	No.5	Precision	Accuracy
Apr.10 (continued)											12.0 12.9 13.1 16.0
Apr.11	3.2×10^4	38.2	41.0	43.2	44.9	48.7	46.7	41.0	45.8		0.0 2.0 2.0 3.9 3.9 4.2 5.2 5.2 6.1 7.0 7.1 5.8 7.8 8.1 9.1 9.1 11.0 11.0 11.9 12.3 13.0 16.1 17.2 17.2 18.1 20.0 24.1

Date	Flux	Al Casting	Al_2O_3	Bramadat's Bauxite	No.1	2D	No.3	4D	No.5	Precision	Accuracy
Apr.16	3.2×10^4				48.6	35.2		33.6			
Apr.18	3.2×10^4	35.4	42.8	44.1	48.3	35.7	41.6	35.5	40.7		

Date	Flux		
Apr.18	R-1751	R-1737	
	42.2	44.8	

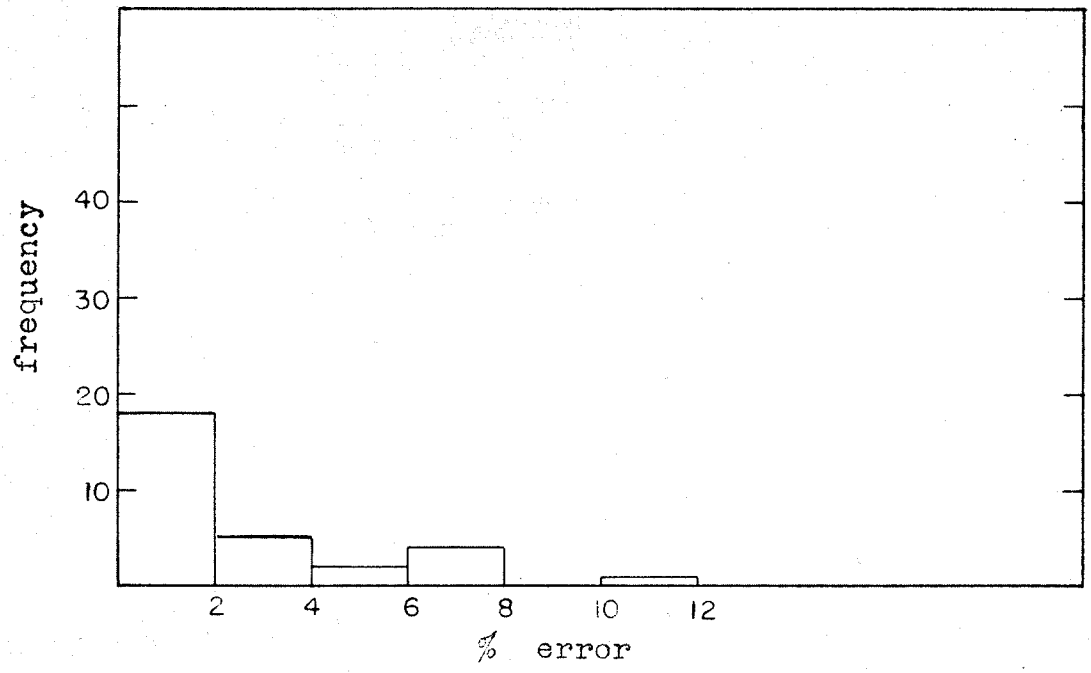

Fig.33 Precision of Al analysis in bauxites

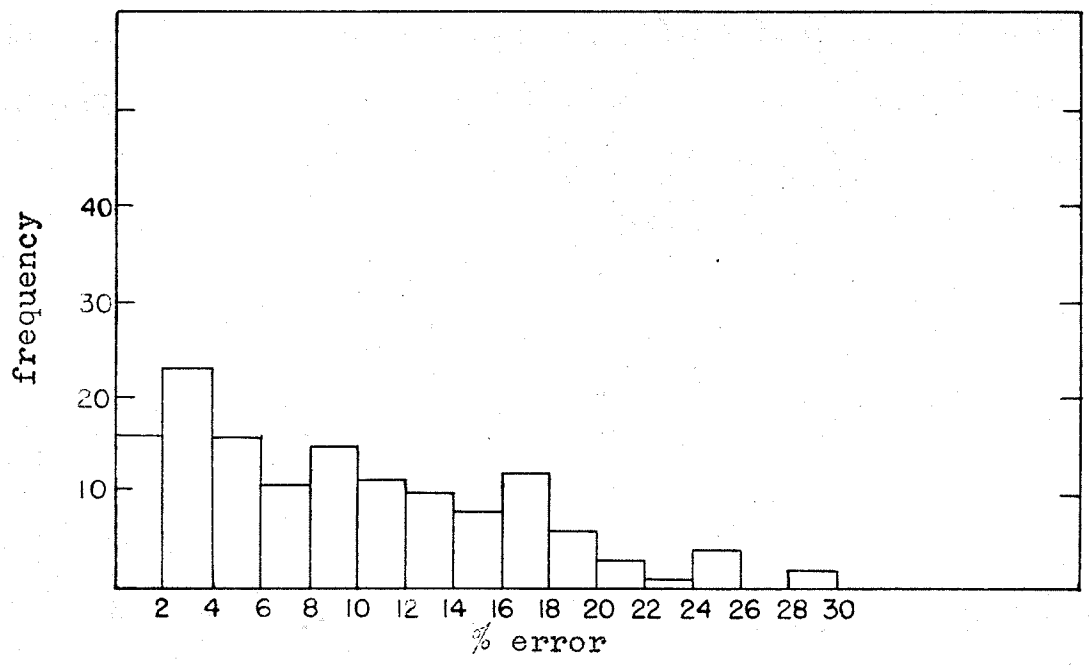

Fig.34 Accuracy of Al analysis in bauxites

PART IV

SODIUM ANALYSIS IN IGNEOUS ROCKS

1. Introduction. Induced radioactivity is a labor saving method for the quantitative analysis of Na in igneous rocks. After crushing, the operation proceeds with only periodical attention from the operator, actually taking less than one-half hour.

2. Method. 300 gm. samples of crushed igneous rock were used, the same as for Al analysis. The background and natural radioactivity was measured for each instrument setting. They were irradiated with slow neutrons overnight (16 hours) and then left for 7 hours. In this time, most of the activity due to the Si, Al, Fe, and Mg content disappeared (see Table 1 Page 26). The longer lived unstable isotopes of Na and K are now the main sources of induced activity. However, the effect of Na will be dominant, by about 17 times that of K, because:

(a) Na^{23} has 100% abundance while K^{41} has 7%.

(b) Na is usually twice as abundant as K in igneous rocks.

(c) K has a cross-section for the thermal neutrons of 1, Na 0.6.

The decay curves of some igneous rocks, showing Na^{24} activity are shown in Fig. 35. Four gamma counting methods were tried.

(a) Integral counting of all energies above 662 Kev

(b) Integral counting of all energies above 1.4 Mev

(c) Differential count of the 1.38 photopeak, gate 1.32 - 1.52 Mev.

(d) Differential count of the 276 photopeak, gate 2.63 - 2.81 Mev.

Methods (a), (b) and (c) have, in that order, the fastest counting rates, and take less than 15 minutes to count. Their disadvantages are, firstly, a high background count, and secondly, the inclusion of other induced activities which are not corrected for. Potassium, and probably Fe, interfere. The fast neutron reaction probably takes place, and gives high results for the high-iron rock R-1767. Method (c) includes the count of the 1.46 Mev photopeak of K. Methods (c) and (d) have the weakness of the low efficiency of the photoelectric effect for high energy gammas. The counting rate is low, and (d) will require a half hour count. The advantage of (d) is that there is no interference. The background is low, and only the Na^{24} 2.76 Mev photopeak is covered. A further advantage in this method is that the 7 hour delay period to eliminate interferring activities can be dispensed with, and in consequence a higher counting rate will be available than that reported in table 10.

3. Experimental data is given in tables 7 - 10, as follows:

Table 7 - method (a)

Table 8 - method (b)

Table 9 - method (c)

Table 10 - method (d)

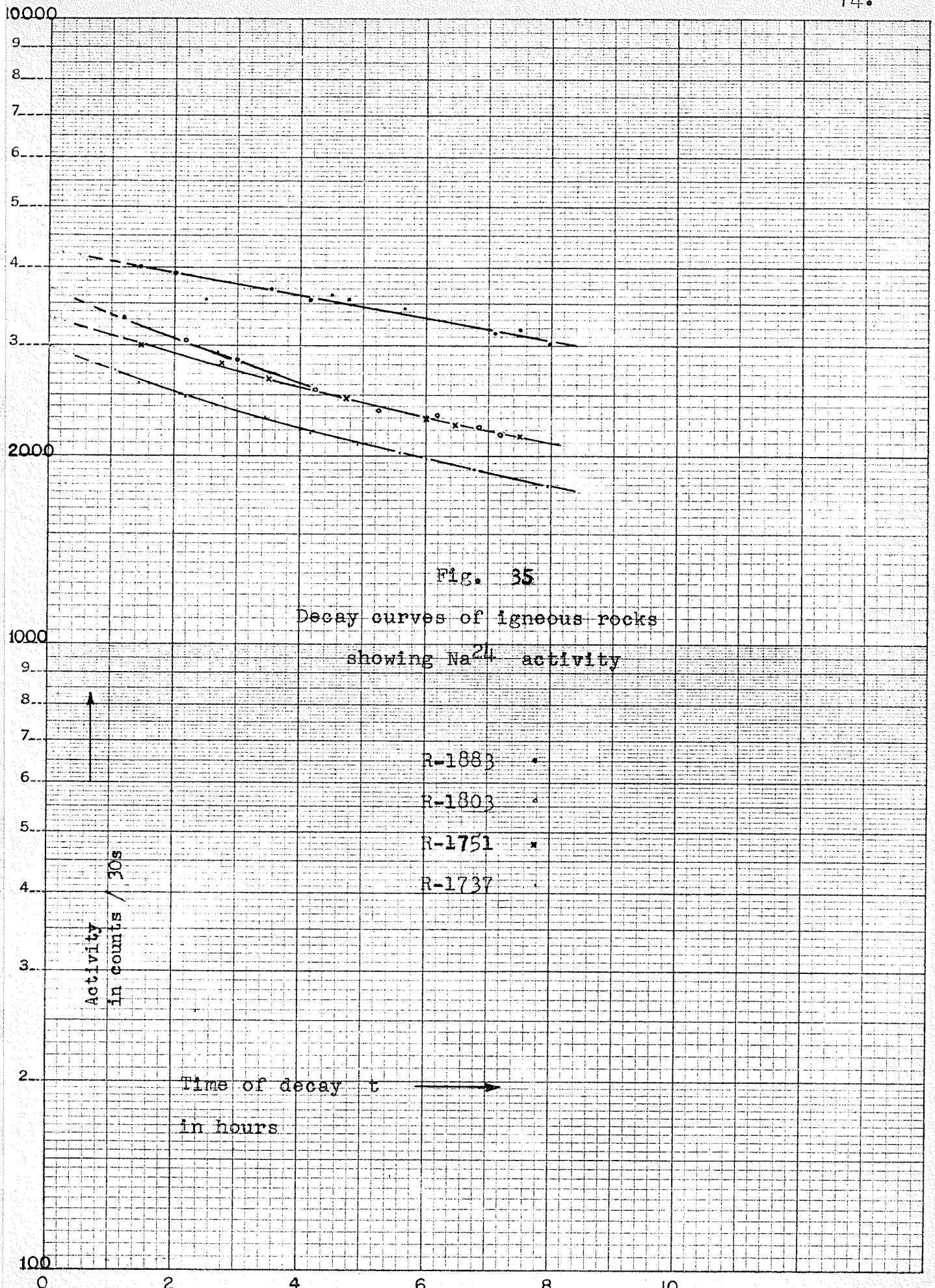

Fig. 35

Decay curves of igneous rocks showing Na^{24} activity

R-1767 gives excessively high results for methods (a), (b) and (c). This rock is exceptionally high in Fe, containing 29% FeO and 5% Fe_2O_3, as shown by table 2.

4. Error. The sources of error are the same as for the Al method in igneous rocks, except for the absence of the errors of graphing and calculation, and the additional errors of interference. The interference of K is small, and did not give noticeable error. The effect of Fe was only noticed in the case of R-1767; however, that it exists is clearly shown in fig. 35. R-1803 and R-1751 have similar amounts of Na_2O, (4.18% and 4.08%), and their decay curves coincide after 4 1/2 hours. Up until that time the curve of R-1803 (8.8% FeO and 6.5% Fe_2O_3) had greater activity than that of R-1751 (6.8% FeO and 1.6% Fe_2O_3), because of the 2.6 hour Mn induced from Fe^{56}.

Method (a) gave results accurate within 11%, with one large exception, R-1767.

Method (b) gave results accurate within 14%, with one large exception, R-1767.

Method (c) gave results accurate within 20%, with one exception, R-1767.

Method (d) gave results accurate within 10%, except for R-1883, which was 15% too low.

TABLE 7

Na analysis in igneous rocks by integral count of induced gamma activity above 0.662 Mev, method (a)

Sample	Activity counts/m	Background	Corrected c/m	Weight Na_2O	c/m/g Na_2O
R-1883	3020	248	2772	18.72	148
R-1883	3133	252	2881	18.72	154
R-1791	1731	252	1479	9.30	160
R-1737	1681	277	1404	8.40	167
R-1751	2355	327	2028	12.24	165
R-1751	2087	211	1876	12.24	153
R-1730	1365	135	1230	7.89	156
R-1803	2125	256	1869	12.54	149
R-1982	1521	180	1341	8.13	165
R-1989	1480	166	1314	8.16	161
R-1767	1051	164	887	3.16	281
R-1767	1122	155	967	3.16	306

TABLE 8

Na analysis in igneous rocks by integral count of induced gamma activity above 1.4 Mev, method (b)

Sample	Activity counts/m	Background	Corrected c/m	Weight Na_2O	c/m/g Na_2O
R-1883	1350	90	1260	18.72	67.3
R-1883	1273	75	1198	18.72	64.1
R-1791	732	67	665	9.30	71.5
R-1737	722	91	631	8.40	75.1
R-1751	1038	187	851	12.24	69.6
R-1751	911	66	845	12.24	69.1
R-1730	599	45	554	7.89	70.3
R-1803	930	84	846	12.54	67.4
R-1803	892	62	830	12.54	66.2
R-1982	626	52	574	8.13	70.7
R-1767	373	41	332	3.16	105
R-1767	363	53	310	3.16	98.1

TABLE 9

Na analysis in igneous rocks by differential count of induced gamma activity 1.32 to 1.52 Mev, method (c)

Sample	Activity counts/m	Background	Corrected c/m	Weight Na_2O	c/m/g Na_2O
R-1883	472	30	442	18.72	23.6
R-1791	268	39	229	9.30	24.6
R-1737	281	30	251	8.40	28.7
R-1751	328	30	298	12.24	24.3
R-1751	374	30	344	12.24	28.1
R-1730	224	23	201	7.89	25.5
R-1982	236	29	207	8.13	25.4
R-1767	127	28	99	3.16	31.3
R-1767	118	28	90	3.16	28.5

TABLE 10

Na analysis in igneous rocks by differential count of induced gamma activity 2.63 to 2.81 Mev, method (d)

Sample	Activity counts/m	Background	Corrected c/m	Weight Na_2O	c/m/g Na_2O
R-1883	174	11	163	18.72	8.69
R-1791	96	10	87	9.30	9.35
R-1737	95	9	86	8.40	10.2
R-1751	137	11	126	12.24	10.3
R-1751	136	12	124	12.24	10.1
R-1730	86	10	76	7.89	9.64
R-1803	141	13	128	12.54	10.2
R-1803	134	9	126	12.54	10.1
R-1982	91	12	79	8.13	9.71
R-1767	43	13	30	3.16	9.49
R-1767	42	10	32	3.16	10.3

5. Conclusions.

Rapid analysis of Na in igneous rocks is feasible by measuring the induced gamma activity. Counting the 2.76 Mev photopeak excludes the interference of other elements. The probable error will be within 15%.

R-1767, a rock exceptionally high in Fe, gave high results in the other methods tried.

The scintillation counter must be checked every day to make sure that the counting rate is constant.

PART V

ALPHA COUNTING

PRELIMINARY EXPERIMENTS

1. Introduction. Alpha counting is a direct, fast, method for the quantitative analysis of U and Th, and is sensitive in trace amounts. Hurley and Fairbairn (1953), Larsen et al (1952), and Kulp, Holland, and Volchok (1952) have used it in geological investigations.

The U content is necessary for the age determination of granitic rocks by the zircon method. It is anticipated that dating parts of granitic rocks will help solve some of the structural and genetic problems of geology, and the zircon method has appealing advantages.

Larsen, Keevil and Harrison (1952) used an age formula which required a trace lead determination and an alpha count. The constant in this formula includes the Pb/U/age constant, the apparatus constant (alpha/U), and to a satisfactory extent, a correction for the Th content.

The zircon method of Holland and Gottfreid (1955), requires an alpha count (or U determination) and a measurement of the structural deformation by X-ray crystallography. His charts convert this data into the solution of the equation ''time x activity equals deformation''. In the structure of zircon, independant SiO_4^{-4} tetrahedra are linked by Zr^{+4} in

8 fold co-ordination. However, the radius-ratio of Zr^{+4} to O^{-2} is theoretically 0.66, which is in the 6-fold coordination ratio range (0.41 - 0.73); therefore the arrangement is not stable and is deformed by radioactivity. Although the atomic radii of U^{+4} (1.05) and Th^{+4} (1.10) are larger than Zr^{+4} (0.87) there is some substitution which makes zircons radioactive.

2. Theoretical considerations.

(a) It is assumed that the U series is in equilibrium.

(b) Th will interfere with these methods. However, Larsen claims that the Th content is small and fairly constant and is satisfactorily corrected for in his equation constant. There are 8 alpha emissions in the U^{238} series, ranging in energy from 4.18 to 7.68 Mev. There are 6 alpha emissions in the Th series, ranging in energy from 3.98 to 8.87 Mev. U^{238} disintegrates 3 times as fast as Th^{232}. Therefore, the U equivalent of Th is

(a) for α activity $\frac{6}{8} \times \frac{1}{3} = \frac{1}{4}$

(b) for Pb content $\frac{1}{3}$

(c) Alpha particles are heavy and easy to stop, they have an atomic weight of 4, and a charge of plus 2. They will not even penetrate a layer of paper and this is the difficulty in counting them. The sample must be as close as possible to a bare phosphor.

(d) The thin layer of phosphor powder will stop the

alphas. Most of the betas and gammas will penetrate the phosphor, and the scintillations that are produced can be discriminated out because they have less energy than the alphas.

3. Apparatus. The same scintillation counter set-up is used, the only change necessary is the phosphor; see fig. 35. For alpha counting, ZnS(Ag) gave the best results. A plastic sheet type was tried, with no success. The idea behind the plastic sheet was that the beta and gamma rays would pass right through and only the alphas would count. Also, the sheet was very convenient for sample application. The powdered sample was simply spread directly on the plastic sheet, and after counting, could be brushed clean. On the other hand, in the use of ZnS(Ag), this powder must be sprinkled on into silicone oil, and the photomultiplier inverted over the sample so that the phosphor will not be contaminated.

4. Procedure.

(a) The detector unit was checked to make sure that it was light tight. The house was made up of a detachable cylinder, fitted on the aluminum base.

(b) The end of the photomultiplier tube was lightly smeared with silicone oil. The powdered phosphor, ZnS(Ag), was sprinkled lightly into this oil.

(c) The alpha emitting sample, ground to a powder, is placed in the sample holder. This is a plate of lucite with a circular depression 1 m.m. in depth. The diameter of

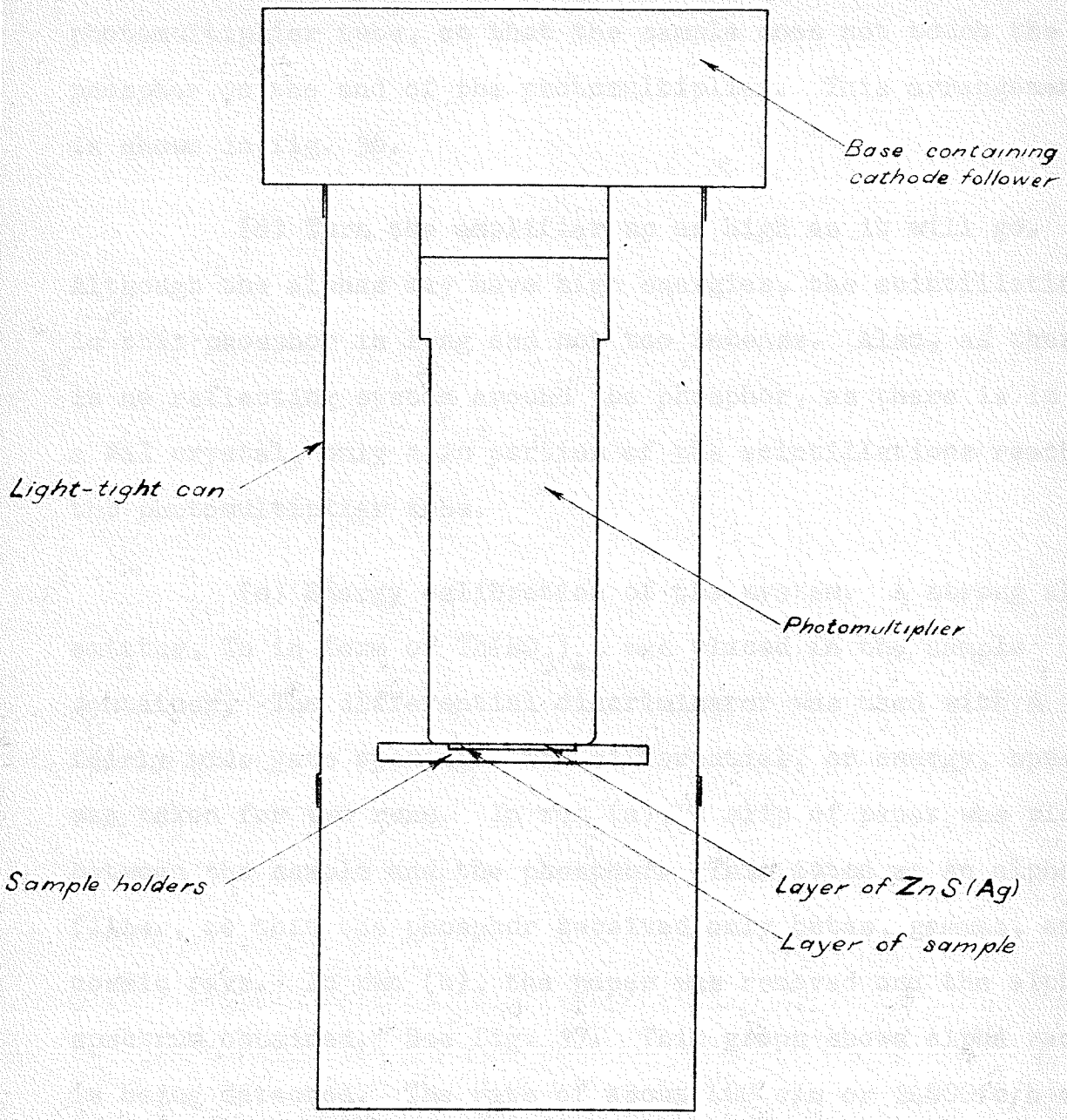

Fig. 36

DETECTION UNIT FOR ALPHA COUNTING

this depression was one quarter inch less than that of the photomultiplier tube, so that the sample does not touch the phosphor on the end of the photomultiplier. This arrangement is shown in fig. 36.

(d) Turn the amplifier up as high as it will go. Although the alphas may have high energies, the scintillation in this phosphor is long and not too intense. Also, as there is no reflecting system around the phosphor, as there is in a NaI crystal, only a 2π portion of the scintillations reach the photomultiplier tube.

(e) Energy calibration of the system. A strong alpha emitter, Th in form of $Th(NO_3)_4$, was placed in the sample container. The differential discriminator was used with a fairly wide gate opening. The differential, or energy, spectrum was taken for two runs. In run (a), a slip of paper was placed between the sample and the phosphor. This acted as an alpha filter, so that the phosphor received only betas, gammas, and cosmic rays. In run (b), the paper was removed and the alpha spectrum obtained. See fig. 37. This graph shows alpha radiation is being detected. The rate of about 400 c/m or 24000 c/h on the differential discriminator would be increased by an integral count, if total alpha count was desired. A significant feature of the graph is the trough at about 0.4 on the bias. This is the upper energy of the gammas and the lower limit of the alphas.

(f) A sample of ground zircon from the mineralogy

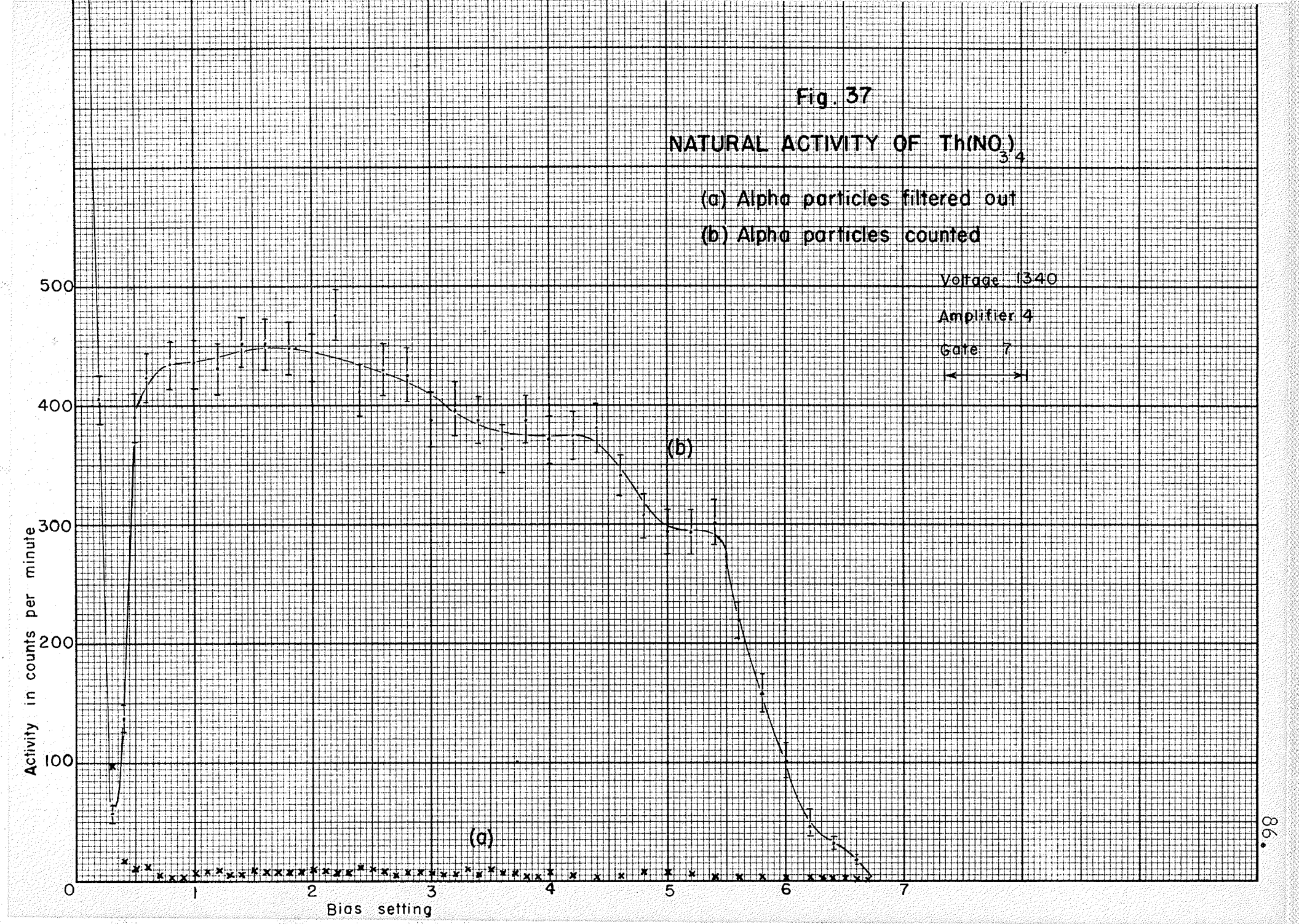
Fig. 37
NATURAL ACTIVITY OF Th(NO3)4
(a) Alpha particles filtered out
(b) Alpha particles counted
Voltage 1340
Amplifier 4
Gate 7
(b)
(a)
Activity in counts per minute
Bias setting
0
1
2
3
4
5
6
7
100
200
300
400
500

museum was placed in the container and covered with an alpha filter. The integral discriminator was set at 0.8 on the dial, so that all counts of energy above this level would be counted. The first run with the alpha filter gave the background at 20 c/h. Then the alpha filter was removed, and the alphas counted for one-half hour at the same settings. The rate was 240 c/h.

5. Results. Crushed zircons, with an assumed U content of about 40 p.p.m., gave an alpha count of 240 c/h. The background, caused by noise and high energy cosmic rays, was 20 c/h., leaving a net activity of 220 c/h.

6. Conclusions.

(a) Sheet plastic phosphor does not work.

(b) Using a ZnS(Ag) phosphor, the alphas from a trace amount of U or Th can be counted at a satisfactory rate.

(c) The rate could be increased by

(1) scanning a larger sample area with the photomultiplier tube, and

(2) grinding the zircons to a finer powder, below 100 mesh.

7. Future problems. The constant relating alpha count to U or Th-U content must be evaluated. The easiest way would be to write to Dr. P.M. Hurley at M.I.T. and ask for some of his measured zircon samples.

REFERENCES

Bramadat, K., (1954), Preliminary Investigations on Activation Analysis; Unpublished Thesis, University of Manitoba.

Holland, H.D. and Gottfreid, D., (1955), the Effect of Nuclear Radiation on the Structure of Zircon; Ac. Cryst. 8, 291.

Hurley, P.M. and Fairbairn, H.W., (1953), Radiation Damage in Zircon: a Possible Age Method; Bull. G.S.A. 64, 659.

Knutson, R.A., (1954), Activation Analysis for Silica in Igneous Rocks; Unpublished Thesis, University of Manitoba.

Kulp, J.L., Holland, H.D., and Volchok, H.L., (1952), Scintillation Alpha Counting of Rocks and Minerals; Trans. Am. Geophys. Union 33, no.1, 101.

Larsen, E.S., Keevil, N.B. and Harrison, H.C., (1952), Method for Determining the Age of Igneous Rocks Using the Accessary Minerals; Bull. G.S.A. 63, 1045.

U.S.A.E.C., Nuclear Science Abstracts; Cumulations for 1952, 1953, and 1954.

Meinke, W.W., (1955), Trace Element Sensitivity; Comparison of Activation Analysis and Other Methods; Science Feb.11, 1955.

Muehlahuse, C.O. and Thomas, G.E., (1950), Use of Pile for Chemical Analysis; Nucleonics 7, no. 1, 9.

Way et al, (1950), Nuclear Data; Circular of the U.S. National Bureau of Standards 499.

Whitmore, B.G. and Baker, W.B., (1950), The Energy Spectrum of Neutrons from a Po-Be Source; Phys. Rev. 78, no. 6, 799.